Assessment of Coal and Petroleum Coke Pollution

Air Quality, Health, and Environmental Justice


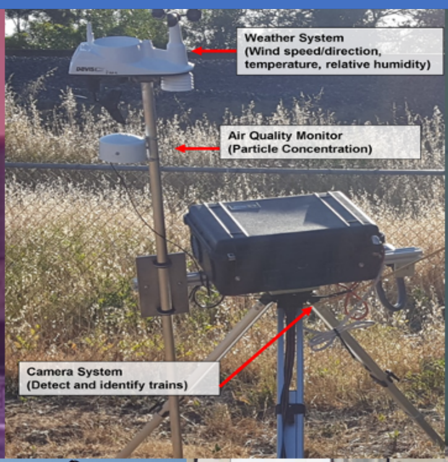

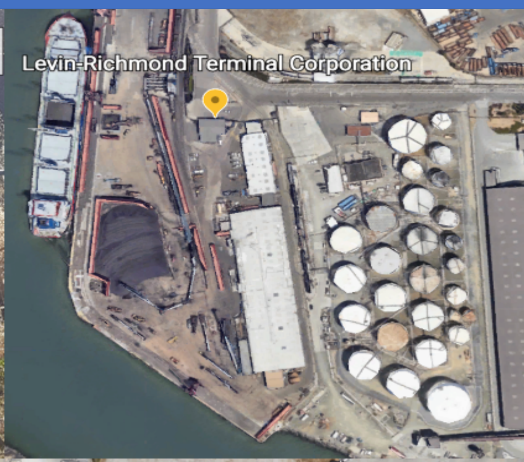


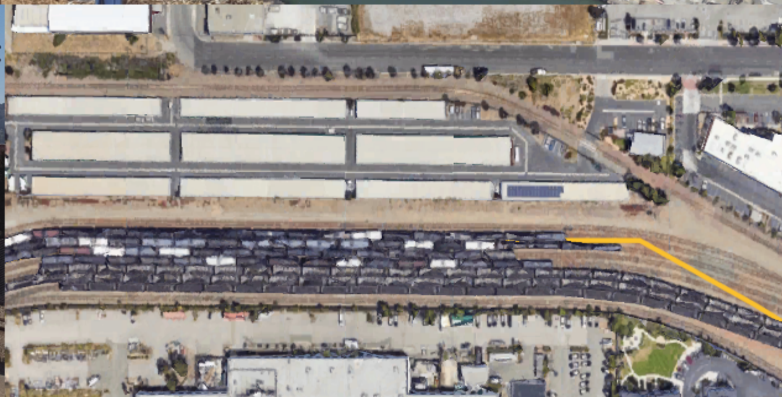

April, 2023

Bart Ostro PhD, Air Quality Research Center, University of California, Davis

Nicholas Spada PhD, Air Quality Research Center, University of California, Davis

Heather Kuiper DrPH, MPH, Independent Consultant

California Air Resources Board Community Air Monitoring Grant: Grant G19-CAGP-17

California Climate Investments
Cap and Trade Dollars at Work

ACKNOWLEDGEMENTS

This work was supported by the California Air Resources Board Community Air Monitoring Grant Program (Grant G19-CAGP-17). The pilot portion of this study was also funded in part by a local community member.

Fiscal Sponsorship of ACAPP was provided by Human Impact Partners, a 501c3 non-profit public benefit corporation. Human Impact Partners mission is to transform the field of public health to center equity and build collective power with social justice movements.

The hosts for our active monitoring sites were indispensable to this project. The City of Richmond's facilitation of our passive monitoring was key to assessing the presence of coal in residential neighborhoods. The support provided to the submission of this grant enabled it to be funded.

Lisa Diemoz and Jessica Cunningham-Krahl of Contra Costa Health Services provided significant health data resources that assist in understanding the health implications of study findings.

Undergraduate student research assistants of the UC Davis Air Quality Research Center provided key contributions to this project. Dhawal Majithia developed the cloud data service system. Garett Roe supported field operations. Hanna Best and Alexa Wells performed image classification for training the computer models.

Salomi Sandhya provided bibliographic assistance.

This report is dedicated to health and stewardship.

TABLE OF CONTENTS

EXECUTIVE SUMMARY

Though coal is transported globally and constitutes a major portion of all rail freight transport, to our understanding, very few studies have quantified the impact of coal rail transport, storage, and handling, particularly in populated urban areas. This knowledge gap is important because these activities contribute to ambient air pollution in the form of fine particulate matter less than 2.5 microns in size ($PM_{2.5}$). $PM_{2.5}$ is known to have significant impacts on both mortality and morbidity. Our study addresses this need for further knowledge by quantifying the ambient impact of rail transport, storage, and handling in a large urban area.

$PM_{2.5}$ is one of the world's leading causes of mortality, accounting for nearly 12% of the global total. $PM_{2.5}$ is causally associated with serious health outcomes and significant healthcare utilization and productivity impacts. The World Health Organization and US Environmental Protection Agency indicate no known safe level of $PM_{2.5}$; current US regulatory standards do not represent a safety threshold. Further, adverse effects result from not only chronic exposure but also exposure as short as one hour. $PM_{2.5}$ additionally constitutes an environmental justice concern because resulting exposure and adverse effects are borne disproportionately by the most vulnerable.

The present study examined the extent to which $PM_{2.5}$ is generated by rail transport of coal as well as by its storage and handling at the Levin Terminal and nearby rail holding yard in the City of Richmond, California. It also considered whether these emissions increase PM2.5 community exposure and related health risks for residents. Specifically, during periods between October 2019 and October 2022, the study measured coal-related $PM_{2.5}$ associated with: 1) rail conveyance of coal through Richmond; 2) coal train car storage at the holding yard; 3) coal and petcoke storage and handling activities at the Levin Terminal; and 4) exposure in nearby communities.

The study has several advantages, including development of an AI-based platform for precise identification of train types during both day and night; siting of monitors and speciation analyses that identify the independent contribution of coal-related pollution; real-time measurement of $PM_{2.5}$ and meteorology; and the ability to produce data on train direction and speed. The novel methods developed for this study overcame barriers to the study of rail activity that make a broader contribution to monitoring mobile and episodic sources of air pollution.

The impact of coal transport storage and handling in urban settings has broad implications, as the resulting dispersion of $PM_{2.5}$ will increase exposure for large populations. Since rail conveyance of coal occurs in populated areas worldwide, it represents a significant local and global public health hazard that extends to matters of environmental and racial justice. Since this activity is for the ultimate purpose of burning fossil fuels, it is relevant to note that these same communities are also at greater risk from the impacts of climate change. Further, recent derailments augment this study's contribution to the general body of knowledge concerning rail activity.

This study found several sources of increased particulate matter related to coal storage, handling, and conveyance. Even so, these increments likely underestimate actual effects as they do not include coarse and ultrafine particles, which also cause adverse health outcomes.

- **Rail conveyance of coal significantly increases ambient concentrations of $PM_{2.5}$.** The average (5-minute) change from passing coal trains adds approximately 8.3 $\mu g/m^3$ (95% CI = 6.4, 10.3) to the ambient $PM_{2.5}$, with midpoint estimates ranging from 5 to 12 $\mu g/m^3$. Full coal cars contribute approximately 2 to 3 $\mu g/m^3$ of $PM_{2.5}$ more than freight trains. With calm winds, the nearby concentrations from coal trains were about 12 $\mu g/m^3$ versus 5 $\mu g/m^3$ for freight trains. Considering only winds from the west resulted in an increase of 25 $\mu g/m^3$ from coal cars. The peak concentration (10 second average) from coal trains was 17.4 $\mu g/m^3$, about 3.5 $\mu g/m^3$ more than freight trains. Calm wind conditions resulted in an increase of 20 $\mu g/m^3$.
- **Rail transit of unloaded cars increases ambient $PM_{2.5}$ concentrations,** adding 2 $\mu g/m^3$ of $PM_{2.5}$, with a range of from about one (non-significant) to over 5 $\mu g/m^3$.
- **Storage of coal and coal cars at the rail yard significantly increases ambient concentrations of $PM_{2.5}$.** Full coal train cars kept at the train yard contribute 2 to 3 $\mu g/m^3$ (one-hour average) of $PM_{2.5}$ above background concentrations, often 0.2 $\mu g/m^3$ greater than those of freight trains. Contribution from full coal cars appears to significantly increase during windier days. Empty coal cars stored at the yards contributed to ambient $PM_{2.5}$ by an increment of 0.2 $\mu g/m^3$ over freight trains during days of relatively calm winds.
- **Terminal operations involving coal transport, storage, and handling, significantly increase community exposure to ambient $PM_{2.5}$** at concentrations ranging from 0.1 to 0.6 $\mu g/m^3$. This presence of coal in the community was independently detected with 1) passive samplers; 2) adhesive carbon tape; and 3) DRUM (Davis Rotating Unit for Monitoring).
- **These $PM_{2.5}$ increments subsequently increase the risk of a wide range of adverse health effects with environmental justice implications** for the exposed population, as the adverse effects are borne disproportionately by the most vulnerable, including infants, children and the elderly, people of color, those with low incomes, and those with underlying health conditions.

Reducing $PM_{2.5}$ can decrease overall mortality risk and also provide larger relative benefits to those with the highest risk, thereby decreasing health disparities while promoting health for all. Studies on specific pollution sources, such as this one, open pathways to emission reductions. We therefore recommend increasing investment in this type of study that integrates AI detection and visualization monitoring with multiple speciation analyses and study designs for targeted assessments to support health, equity, and environmental justice.

1. Introduction

AB617 aims to improve air quality in environmental justice communities through local, community-specific strategies focused on the individual needs and issues particular to each community. Our study, Assessment of Coal and Petroleum Coke Pollution (ACAPP), serves this goal by focusing on harmful particulate matter air pollution in the City of Richmond, CA, a designated AB617 environmental justice community. ACAPP assesses the extent to which specific local activities (coal transport by rail, coal and petcoke storage and handling at the terminal) emit particulate matter and considers potential health implications for the local community. By using data and analytical methods that specifically characterize the role of rail and terminal activities, ACAPP contributes to efforts for emissions reductions that will directly benefit the local community.

1.1 Particulate Matter and Health

Myriad large epidemiological studies definitively establish that exposure to fine particulate matter (particles less than 2.5 microns in diameter or $PM_{2.5}$) is associated with a wide range of adverse health effects. Exposure to $PM_{2.5}$ has been linked to premature mortality, cardiovascular, cerebrovascular, and respiratory diseases, other chronic diseases, adverse birth outcomes, and cognitive and developmental impairments (WHO 2021; U.S. EPA 2019). These effects occur even at concentrations lower than current regulatory standards (Brunekreef et al. 2021). While most studies of $PM_{2.5}$ have examined daily or multi-year exposures, there is evidence of health effects from exposures of as short as one hour (Liu et al. 2021; Peters et al. 2001; Wu et al. 2020). The World Health Organization recently lowered their threshold guidelines and indicated there is no known safe level of $PM_{2.5}$ (U.S. EPA 2019; WHO 2021). The recent Global Burden of Disease study estimates that exposure to $PM_{2.5}$ contributed to an annual 6.7 million deaths worldwide, nearly 12% of the global total and the fourth-highest risk factor for global mortality (Fuller et al. 2022). Of note, exposure to $PM_{2.5}$ constitutes an environmental justice concern as exposure and adverse effects are borne disproportionately by the most vulnerable, including infants, children, the elderly, people of color, those with low incomes, and those with underlying health conditions (Tessum et al. 2021).

1.2 Fossil Fuel and Particulate Matter

Recent studies report that the combustion of fossil fuels, including coal, oil, and natural gas, is the largest source of ambient $PM_{2.5}$-related mortality, accounting for nearly 9 million premature deaths among adolescents and adults, roughly 1 in 5 of all deaths, with additional, heightened mortality burdens among children (McDuffie et al. 2021; Vohra et al. 2021). Combustion, however, is not the only source of coal-related particulate matter as fugitive dust from rail transport is known to be significant (BNSF Railway 2011; Vohra et al. 2021). As demonstrated by Jha & Muller (2018), "Coal does not have to be burned to have an impact on the local environment and the health of residents," suggesting that mortality and adverse health burdens of fossil fuel $PM_{2.5}$ are even greater than described.

1.2.1 Transport

Rail conveyance is an additional source of coal-related particulate matter as fugitive dust from rail transport is known to be significant (BNSF Railway 2011). Trains transport nearly 70% of coal deliveries in the United States (US Energy Information Administration 2022), with coal accounting for 1 of every 3 tons of American rail freight. In a note to its customers, the BNSF Railway's own assessment stated, "The amount of coal dust that escapes from PRB [Powder River Basin coal in Wyoming and Montana] is surprisingly large" (BNSF Railway 2011). BNSF studies indicate 500 lbs. to a full ton of coal can escape from a single loaded car and other reports indicate as much as 3% of coal loaded into a rail car can be lost in transit, even as there is some variability related to various factors such as the weather (Baruya 2012; BNSF Railway 2011). These estimates suggest coal conveyance is a significant contributor to air pollution, and yet quantification of coal train contribution to ambient $PM_{2.5}$ is poorly documented. Given a dearth of studies quantifying the effects of coal transport on subsequent concentrations of particulate matter and the significant health implications of exposure to $PM_{2.5}$, additional study is warranted.

1.2.2 Storage and handling

Coal and petroleum coke storage and handling are a source of fugitive dust emissions by way of fuel loading and unloading, wind erosion, and pile maintenance. These emissions may have significant adverse health implications. The Jha and Muller (2018) study of $PM_{2.5}$ from coal storage piles found that a 10 percent increase in atmospheric $PM_{2.5}$ per cubic meter due to coal dust raised average adult mortality rates by 1.1 percent and average infant mortality rates by 6.6 percent among residents within 25 miles of a coal pile (40.2 km). While not specific to trains and terminals, multiple studies of $PM_{2.5}$ concentrations and dispersion from open-cast coal mines suggest fugitive dust in urban settings will reach residential neighborhoods. For example, Sahu and Patra (2020) reported only a 26% reduction in $PM_{2.5}$ concentrations at 500 meters downwind of coal mine operations, suggesting that the full dispersion range may be extensive.

1.3 Environmental Justice

Identifying the source of fugitive dust is important because the implications of exposure extend beyond individual and population health effects to matters of environmental and racial justice. In other words, understanding the source gives information about equity. In the case of coal and petroleum coke dust from transport, storage, and handling, impacts are especially borne by those in relative proximity to the source facilities, such as tracks, terminals, and holding yards. For example, Jaffe et al. (2015) found that residences 25-30m from rail facilities experienced 6.8 $\mu g/m^3$ higher concentrations of $PM_{2.5}$ than other locations; the outer limits of coal exposure may reach 25 miles (Jaffe et al. 2014; Jha & Muller 2018). This increased exposure compounds health risks because residents in proximity to fossil fuel activity generally are already disproportionately burdened by social risk factors for health, including lower incomes and educational attainment (Davis 2011; Jha & Muller 2018). These and other characteristics of susceptibility and vulnerability qualify such locations as "disadvantaged" or "environmental justice" communities, defined by the California Health and Safety Code Section 39711 as low-income and disproportionately affected by environmental pollution and other hazards.

The coal impacts extend beyond terminal community effects since rail conveyance traverses thousands of miles, exposing multiple environmental justice communities, rivers, and coastlines as the rails trace their contours and culminate on their shores. The climate change implications of coal transport, storage, and handling also have racial and environmental justice impacts. For example, factoring in the ultimate combustion of coal-related transport brings rail transport up to 16% of US carbon pollution (Meyer 2019), with people of color, children, the elderly, and those with low incomes and underlying health conditions disproportionately harmed by resulting climate change impacts (IPCC 2022).

1.4 ACAPP Contributions

To determine the $PM_{2.5}$ concentration resulting from passing full and unloaded ("empty") coal, freight, and passenger trains as well as from storage and handling of coal and petcoke, ACAPP conducted a multi-site study over an extended period, October 2019 to October 2022, in the City of Richmond, California. This study has several strengths that make its findings of use to polic and its methods also contribute to the larger enterprise of pollution monitoring, especially related to mobile sources and episodic pollution events. For example, the study:

- Undertook a comprehensive approach by assessing pollution related to coal transport, storage and handling, as well as community exposures. Monitoring sites were maintained and utilized at a rail corridor site, a rail car holding yard site, two sites at the Levin Terminal, four neighborhood sites, and four control sites, for a total of 13 sites.
- Monitored several locations for an extended period, thereby increasing the statistical power and robustness of the estimation of impacts by increasing the number and characterization of measured increments.
- Deployed design and analysis techniques that enabled identification of the sources of pollution increments, which is often difficult to isolate in urban environmental justice

communities, which are burdened by multiple pollution sources. Specifically, it did so by citing monitoring stations in locations unimpacted by other emission sources, incorporating control measures that similarly ruled out other sources, and incorporating speciation analysis to ascertain the nature of the particles measured.

- Pioneered the use of an AI-driven algorithm, incorporated infrared night-vision to ascertain the independent effects of both empty and loaded coal trains as compared to freight trains and passenger trains, and increased data quality by enabling the detection of a large number of coal trains.
- Deployed superior monitoring mechanisms that included a custom package of three optical PM sensors (PMS5003, Nanchang Panteng Technology Co., Ltd, China), commonly recognized as the sensors used in the widely-distributed PurpleAir PA-II monitor (Ouimette 2022). The sensors' high temporal resolution of one second and their inter-instrument precision enabled the detection of rapid train events. Additionally, the train monitoring system comprised three data collection systems: a personal weather station, an air quality sensor, and a computer-vision system, and enabled the incorporation of meteorological information, train direction, and speed.
- Applied strong quality control measures in data management. These included data quality metrics of the $PM_{2.5}$ data for 1 second, 10 seconds, and 10 minutes, equivalent to instantaneous readings, train event averaging, and pre-event background conditions, respectively. In addition, multiple monitor channels were utilized, compared to a typical two, to strengthen data quality control and calculate variance for each observation. Prior to evaluation, the data were cleaned to remove aberrant sensor readings.

Also of significance, by successfully monitoring rail activity in a densely-populated urban setting, the present study produces findings that are directly relevant to assessing health impacts and making policy decisions, both by incorporating the relevant emission conditions (e.g., effective wind speed) and by characterizing the communities typically in proximity to rail and terminal settings, thereby making it directly relevant to not only fossil fuel particulate matter exposure but also to environmental justice. It is important to note that our analysis did not include measurements of either ultrafine (particles less than 0.1 microns) or coarse particles (PM10), which are generated along with $PM_{2.5}$. Since there is substantial evidence of adverse health effects from these additional particle sizes, the exposures and health risks identified in this study are underestimated.

1.5 Report Overview

This report contains four sections:

- **Section 2** analyzes the $PM_{2.5}$ increment from passing trains, including full coal cars, unloaded coal cars, freight cars, and passenger cars.
- **Section 3** examines the $PM_{2.5}$ increment from the coal and freight cars at the train holding yards about one mile from the export terminal.
- **Section 4** provides the results of the measurements of coal and petcoke $PM_{2.5}$ emanating from coal terminal operations in the surrounding neighborhoods.
- **Section 5** describes the implications for subsequent health impacts and environmental justice concerns in Richmond and Oakland.

A list of references and appendices follows these sections.

2. Coal-related $PM_{2.5}$ effects from coal trains

Trains transport nearly 70% of coal deliveries in the United States, with coal accounting for 1 of every 3 tons of American rail freight (US, Energy Information Administration 2022). In a note to its customers, the BNSF Railway's own assessment stated: "The amount of coal dust that escapes from PRB [Powder River Basin coal in Wyoming and Montana] is surprisingly large," and reports have indicated that as much as 3% of the coal loaded into a coal car can be lost in transit (Baruya 2012; BNSF Railway 2011). Studies have confirmed that coal trains produce particulate matter through not only engine diesel emissions but also directly from coal. These latter emissions are via blow-off, suspension, and re-entrainment from wind erosion and wind scouring of loaded and unloaded coal cars, door leakage, and the "parasitic load," i.e., coal spilled and carried on external parts of the train (Prakash et al. 2018). The magnitude of ambient particulates from coal trains is influenced by train and wind speed, weather, moisture, rail car and load geometry, physical properties of the coal, vibration, and the use and efficacy of dust suppression methods (Prakash et al., 2018). Unfortunately, the actual contribution of coal trains to ambient $PM_{2.5}$ is poorly documented.

Given the dearth of studies quantifying the effects of coal transport on subsequent concentrations of particulate matter and the significant health implications of exposure to particulate matter, additional study is warranted. Below, we report results from the novel monitoring system we developed and utilized to quantify the contribution to ambient $PM_{2.5}$ from uncovered railcars that convey coal predominantly from mines in Southern Utah to the Levin Terminal in Richmond, California.

2.1 Methods and Materials

2.1.1 Data collection

Particulate matter from coal contains many impurities and elements, including heavy metals known to be toxic or carcinogenic to humans (OEHHA 2015). Specifically, the coal of interest in this study originated from the Wasatch Plateau coal fields, a coal-bearing outcrop approximately 145 km long and 11 to 32 km wide (Hatch et al. 1979). Previous assessments have determined coal from the plateau to be highly volatile bituminous (Hatch et al. 1979). The coal is primarily carbonaceous with various inclusions and impurities, including several mineral species and elemental Cr, Ni, and Se impurities. Trace elements include As, Ba, Cd, F, Mn, Sb, Sr, Th, U, and V (Hatch et al. 1979).

To determine the $PM_{2.5}$ concentration from passing full and unloaded ("empty") coal, freight, and passenger trains, passing trains were monitored from May 19, 2022, through October 31, 2022, at a populated residential site approximately 7 km north of the terminal. The site is near the culmination of an 800-mile journey, thereby capturing the realistic conditions of long-haul coal conveyance compared to the conditions at departure, where dust suppressants are freshly applied and trains are optimally loaded. The monitoring site is approximately 21.5 meters east (generally downwind) of the rail line, with parkland to the east and the San Francisco Bay to the west (Figure 2.1). The site was selected to avoid $PM_{2.5}$ from other important sources, such as major roadways, industrial facilities, Richmond port operations, and the Levin terminal. This location and our study methodology ensured that any observed changes in $PM_{2.5}$ as the trains passed were strictly due to the trains themselves.

Figure 2.1 Monitoring site with amplified detail of equipment and AI-detected coal train

Commercially available motion detection and camera systems were explored for use, but the detection of passing trains was unreliable and the data collection was too cumbersome for long-term monitoring. Therefore, a custom detection system was developed and deployed. The train monitoring system comprises three data collection systems:

1. A personal weather station
2. An air quality sensor
3. A computer-vision system

The personal weather station was selected for direct data output via serial communication (VantageVue, Davis Instruments, USA). It provided wind speed/direction, temperature, ambient pressure, relative humidity, precipitation, and other meteorological parameters. The meteorological data were collected every one minute. In addition, hourly wind speed and direction were retrieved from the NOAA site in Richmond for comparison (Point Potrero 998477-99999).

The air quality sensor is a custom package comprising three optical PM sensors (PMS5003, Nanchang Panteng Technology Co., Ltd, China). These are equivalent to cell-reciprocal nephelometers and are commonly recognized as the sensors used in the widely-distributed PurpleAir PA-II monitor (Ouimette 2022). The sensor responds to optical scattering from a 657 nm laser. Therefore, it is associated with mass via the mass scattering coefficient, a function of the observed particles' chemical, morphological, and optical properties. The accuracy of this determination is governed by the variability of particle characteristics in the temporal and spatial dimensions. The sensors' high temporal resolution of one second and their inter-instrument precision, as assessed by numerous field and laboratory studies, were the principal qualities that enabled the detection of rapid train events (Tsai 2020; AQ-SPEC 2022). Three channels were included to strengthen data quality control and calculate variance for each observation. The raw data from all three sensors were collected every second.

Data quality metrics of the $PM_{2.5}$ data were evaluated for 1 second, 10 seconds, and 10 minutes, equivalent to instantaneous readings, train event averaging, and pre-event background conditions, respectively. Prior to evaluation, the data were cleaned to remove aberrant sensor readings. Specifically, values outside two standard deviations were omitted. These values were excessively high readings from the low-cost sensor in all cases. The observations in the subsequent statistical analysis ranged from 0 to 117.45 $\mu g\ m^{-3}$ with a median uncertainty of 27%, well within the linearity range of the sensors of < 300 μg^3 (Barkjohn et al. 2022).

The computer-vision system consists of a microcomputer (Jetson Nano, Nvidia, USA), a camera (NoIR PiCamera, Raspberry Pi), an artificial intelligence (AI) accelerator (Coral Edge TPU, Google, USA), a solid-state hard drive (500 GB T5, Samsung, S. Korea), and an infrared floodlight (IR Illuminator 30 deg, Axton Technologies, USA). The system was placed approximately 60 meters from the chosen source and operated autonomously on a continuous basis, except for a daily 30-minute period when data was being uploaded to a cloud server (Lightsail, Amazon Web Services, USA).

The computer-vision system is the pivotal technology that enabled the detection of passing trains. Images from the camera were passed to the computer at 30 frames per second, pre-processed, and passed to the AI accelerator. The accelerator is a Tensor Processing Unit (TPU, Coral Edge TPU, Alphabet, USA), which runs an image classification model customized for the monitoring location. This model identified whether or not a train was present in the image. If so, the computer created a train event and recorded: one second before the train was detected, the entire train event, and one second after the train was no longer detected. This recording was saved to an external hard drive as an individual train event. Train speed (MPH) and the train direction towards or away from the terminal were determined during manual post-processing of the data. Determining object velocity from video recordings is error-prone due to variable image processing rates. Train speeds were estimated using the average frame rate (frames per second) recorded during the monitoring period and fixed observation points in the camera's field of view. A schematic diagram of the system is presented in Figure 2.2.

Figure 2.2 Schematic of the rail corridor monitoring system

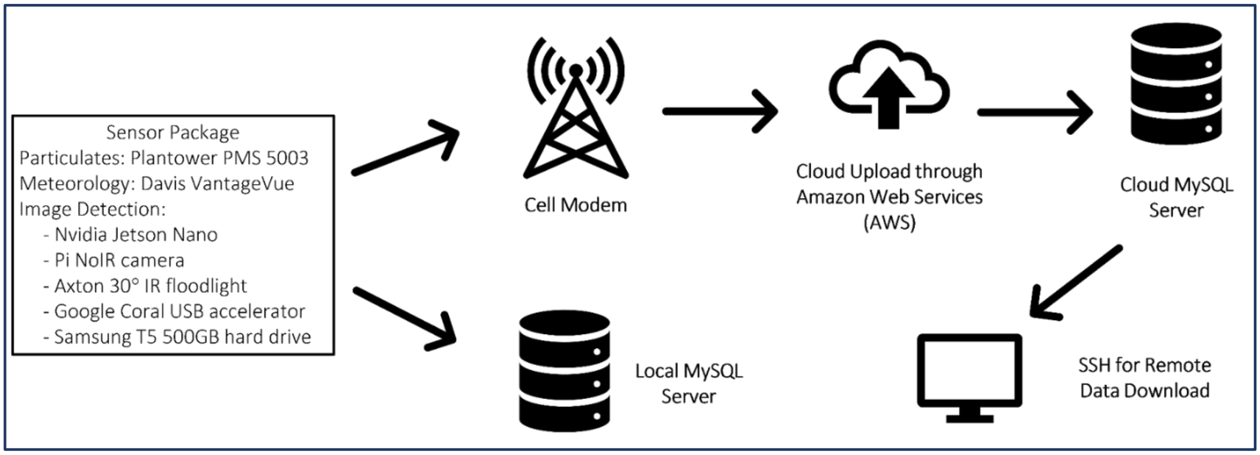

Detection of passing trains relied on an accurate image classification model. Training images were collected at the monitoring site during an initial survey of the rail line. Images were continuously collected every one minute until a suitable number of images were retrieved for each classification: day train, night train, day no train, night no train. The open-source Google MobileNet V2 neural net model was retrained with 174 images of each classification in the top 50 nodes and then fully quantized for operating in TensorFlow Lite on the Google Coral TPU accelerator (int8). Accuracy was controlled at > 90 % for all classifications. In general, daytime classifications were > 98 %, and nighttime classifications were > 90 %.

For each 24-hr period, data was aggregated from all three data sources and standardized into one-second observations for each measurement parameter, including meteorology, $PM_{2.5}$ concentrations, and train detection. During this < 30-minute period, the monitoring systems were disabled and the data file along with associated video files were uploaded to the cloud server. The data aggregation and upload period were scheduled in the early morning hours when train activity was determined to be consistently absent based on initial surveys of images collected every one-minute from the monitoring site. Files located in the cloud were retrieved periodically for post-processing, which consisted of associating particulate matter and meteorological data with the observed train events based on the shared data timestamps. Accurate date and time determinations were ensured by consistent internet connection and verification by the operating system. Further detail on the derivation of the variables used in our analysis is provided in Appendix 1.

2.1.2 Data management

The $PM_{2.5}$ during train passage was recorded in one-second concentrations and averaged for roughly 4 to 5 minutes of passage (longer for freight trains). In addition to the $PM_{2.5}$ average during the passage of the train, the maximum 10-second average concentrations during the train passage were also recorded and analyzed to compare with previous studies.

To determine the change in $PM_{2.5}$ due to passing trains, we quantified the difference between the measured $PM_{2.5}$ at the rail site and a "control" exposure period. The control, also considered a "pre-exposure" period, corresponded to the period just prior to a train's passage, allowing capture of ambient $PM_{2.5}$ without the train's contribution as well as controlling for normal diurnal and regional changes in $PM_{2.5}$ concentrations. Previous studies used a similar approach (Jaffe et al. 2015; Akaoka et al. 2017). We also established a gap between the control period and the train passage to ensure that particles influenced by the high-pressure zone in front of an oncoming train would not be included in the control.

To select the duration of the control exposure and this gap immediately before the train passage, we examined several alternatives, including: a five-minute average ending with a 2- minute gap before the train (5/2) as well as 3/2, 5/5, 10/2, 10/5 and 10/10. Ultimately, the results were insensitive to the alternative control and gap periods, so only the results using 10/10 are reported below, as described in Figure 2.3.

Figure 2.3 Schemata of protocol for calculating change in $PM_{2.5}$ from passing trains

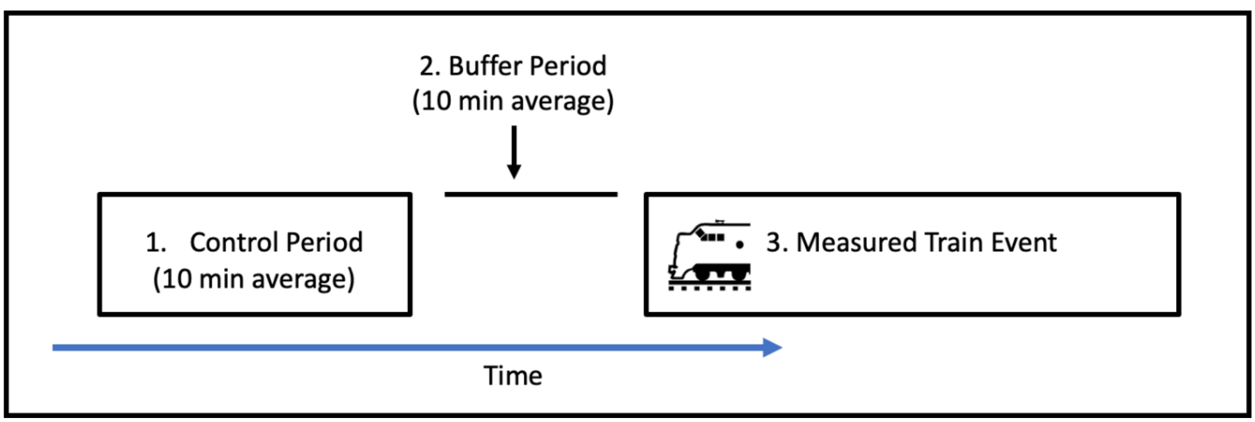

2.2 Analysis

We addressed several issues, including whether full or empty coal cars contribute to local ambient $PM_{2.5}$ concentrations and, if so, by how much. We also compared the impacts of coal cars relative to those of both freight and passenger trains. Using multiple linear regression with the change in $PM_{2.5}$ concentration as the dependent variable, our model included binary variables for each of the four train types (passenger, freight, empty, and full coal) and examined and controlled for potential confounders. For example, a previous study found a strong association between $PM_{2.5}$ from coal trains and the effective wind speed (the sum of train and wind speed) (Jaffe et al. 2015). To test the sensitivity of our results to the model specification, we examined the impact of several covariates, including train speed, wind speed, effective wind speed, duration of exposure (based on the elapsed time of the train passing), average temperature, dewpoint, and relative humidity. The inclusion of humidity served to control for the potential impact of the hygroscopic property of fine particles when measured with optical sensors. We ran the model without a constant term, facilitating the direct comparison of the impact among the train types. The model results were identical to a model that adds a constant term, which drops one of the train types to avoid multi-collinearity.

Additional sensitivity analysis included examining the impact of converting the negative values for the change in $PM_{2.5}$ into zero values. The negative change from the control period could result from significant dust from activities at the monitor's residential location, dust from trains occurring in the control period, or a sudden change in wind speed or direction prior to the train's arrival. We also considered subsets of certain covariates. For example, we examined those days where the wind was below the mean level of 3.1 meters per second (m/s) since these calmer periods may relate to higher concentration at the nearby monitor, whereas particles may disperse to a larger area under other wind conditions. Finally, we tested a model where the air quality sensor was calibrated and directly corrected for relative humidity using our site's closest Federal Equivalency Method (FEM) monitor. This monitor was located in nearby San Pablo (Air Quality System Site ID: 06-013-1004), 1.6 km from our site, and generated the following fit with an R^2 of 0.58:

$$PM2.5\_C = 9.79 + .76 * PM\_PA - 0.095 * humidity$$

Where PM2.5_C is the calibrated and corrected concentration of $PM_{2.5}$, and PM_PA is the original reading at the train site. In addition to the average change in $PM_{2.5}$ (difference of $PM_{2.5}$ during train passage and the control), the maximum (10 second average) concentration relative to the control period was analyzed to compare with the findings of previous studies.

2.3 Results

Ultimately, during the six-month observation period, the increases in ambient $PM_{2.5}$ concentrations were measured during the passage of four different train types. Complete data were available for full coal trains (n =15), empty coal trains (n =14), freight trains (n = 568) and passenger trains (n = 2235), as identified by the video recordings from the camera system described above. There were some significant differences between the characteristics of the train types (see Appendix 2 for detailed summary statistics). For example, focusing on freight trains versus full coal trains, the mean duration (in seconds) and speed (m/s) for the former were 236 and 18.3, vs. 144 and 12.5 for the latter. At the other extreme, the means of these same parameters for passenger trains were 2.2 seconds and 31.7 m/s.

The results for the basic regression model are presented in Table 2.1. As expected, wind and train speed were both statistically significant. In addition, the passage of an empty coal car contributed about 2.3 μg/m^3 (95% CI = -0.28, 4.82; $p < 0.1$) to the ambient air, while freight and full coal cars contributed 4.5 μg/m^3 (95% CI = 3.82, 5.18; $p < 0.01$) and 6.8 μg/m^3 (95% CI = 4.34, 9.24; $p < 0.01$). Controlling for the direction of the freight train did not alter the results. This finding indicated that the regression coefficients of these three train types (freight and full/empty coal) were significantly different from zero and also from each other. In contrast, the $PM_{2.5}$ increment from passenger trains was relatively small and not significantly different from zero, so it was not included in the sensitivity analysis. The amount of explained variation from the basic model was relatively low at 16%. Given the null impact of passenger trains, further results for this mode were not included.

Table 2.2 displays the results of the alternative models of coal and freight train effects.

Table 2.1 Regression results of basic model

Variables	PM2.5avg	PM2.5max
Windspeed	-0.256*** (0.0628)	-3.865*** (0.742)
Train speed	0.0131** (0.00582)	0.185* (0.089)
Passenger	0.257 (0.455)	7.785 (7.265)
Empty Coal	2.274* (1.301)	12.179 (8.194)
Freight	4.496*** (0.347)	18.498*** (4.095)
Full Coal	6.794*** (1.252)	22.838*** (7.484)
R2	0.16	0.18
n	2829	2237

Note: PM2.5avg = average during train passage; PM2.5max = maximum 10 second during train passage; standard errors in parentheses. *** p<0.01; ** p<0.05; * p<0.1

Table 2.2 Regression results of the increase in average $PM_{2.5}$ (5 min avg, µg/m^3) in alternative models

Train type	(1)	(2)	(3)	(4)	(5)	(6)	(7)
Empty Coal	2.27*	5.64***	0.96	5.84***	2.19	3.26	6.41***
Freight	4.50***	7.49***	2.78***	7.80***	5.07***	4.77***	6.53***
Full Coal	6.79***	9.71***	5.09***	10.00***	12.12***	25.00***	8.32***
R^2	0.16	0.16	0.16	0.16	0.19	0.25	0.53
n	2829	2829	2829	2829	1330	627	2829

Models are: (1) Basic (2) Basic + temperature (3) Basic + humidity (4) Basic + dew point (5) wind speed < mean (6) basic + wind speed < mean + west wind (7) Calibrated monitor. (Note: Basic model includes wind speed, train speed and a binary variable for each train type, no constant)

Model (1) reproduces the results of the basic model. Model (2) added the average temperature during the one-hour average that included the train pass and resulting in increases in the $PM_{2.5}$ impact for all three train types, with empty coal, freight, and full coal cars contributing 5.6 µg/m^3 (95% CI=2.5, 8.7), 7.5 µg/m^3 (95% CI = 5.8. 9.2) and 9.7 µg/m^3 (95% CI = 6.8, 12.6), respectively, with all three significant at $p<0.01$. All were statistically significant with $p < 0.01$. Model (3) indicates the impact of adding humidity, resulting in reductions of approximately 2.5 µg/m^3 from the basic case. Model (4) adds a control for dewpoint, a combination of temperature and humidity, which resulted in an increase in the change in $PM_{2.5}$ from the basic model.

Next, in Model (5), observations are restricted to those occurring during calm wind conditions (less than the mean of 3.0 m/s). This constraint significantly increased the contribution of coal trains to ambient $PM_{2.5}$ to 12.1 µg/m^3 (95% CI = 7.7, 16.5; $p < 0.01$) versus 5.1 µg/m^3 (95% CI = 3.8, 6.4; $p < 0.01$) for freight cars. Model (6) adds a restriction by considering only when winds are from the west, the dominant wind direction for this region. This criterion increased the coal contribution to 25 µg/m^3 (95% CI = 17.7, 32.2), while the increase due to freight cars remained close to 5 µg/m^3. However, only 3 coal cars met this criterion.

Table 2.3 Regression results of the increase in peak $PM_{2.5}$ (10 sec avg, µg/m3) in alternative models

Train type	(1)	(2)	(3)
Empty Coal	12.8	9.26	8.09
Freight	18.50***	14.06***	14.37***
Full Coal	22.84**	17.37**	19.96 **
R^2	0.25	0.25	0.27
n	550	550	360

Models are: (1) Basic (2) Calibrated monitor (3) Calibrated monitor with wind < mean.

Note: Basic model includes wind speed, train speed and a binary variable for each train type

*** <0.01; ** <0.05; * <0.1

Finally, Model (7) uses the data from the calibrated $PM_{2.5}$ concentrations and generated statistically significant estimates of 8.3 µg/m^3 (95% CI = 6.4, 10.3; $p < 0.01$) and 6.5 µg/m^3 (95% CI = 6.0, 7.1; $p < 0.01$), respectively, for full coal and freight trains.

Models (1) through (5) each exhibited a modest R^2 of less than 0.19. However, the calibrated Model (7), which provided a robust correction for humidity, explained 53% of the variation in the change in $PM_{2.5}$. Additional model specifications of Model (7) with covariates used in the earlier models, such as train duration, effective wind speed, or quadratic terms, failed to improve the model fit.

Table 2.3 displays the regression results for the increase in peak (10-second average) $PM_{2.5}$ concentrations above the control concentrations during the passing of full coal cars (n = 18), empty coal cars (n = 16), and freight cars (n = 653). Results for passenger trains were not included since they had little impact on $PM_{2.5}$. The model specifications were similar to those used in the previous analyses and included wind speed, train speed, and the 3 train types. Given the above findings, we focused on 3 different models: a basic model (Model 1), a model corrected and calibrated for humidity as above (Model 2), and the calibrated model under calm wind conditions defined as average wind less than the mean (Model 3).

For the basic model, the results indicated an increment in maximum $PM_{2.5}$ over the control period of 22.9 µg/m^3 (95% CI = 8.1, 37.5); $p < .01$) for full coal trains. For the model calibrated and corrected for humidity, the increment from coal cars was 17 µg/m^3 (95% CI = 6.2, 28.5; $p < 0.01$), while the corresponding change in $PM_{2.5}$ was 14.1 µg/m^3 (95% CI = 7.9, 20.2; $p < 0.01$) for freight trains and 9.3 µg/m^3 (95% CI = -3.0, 21.5, NS) for empty coal cars. Under calm wind conditions, the impact from coal cars increased to almost 20 µg/m^3 (95% CI = 3.4, 36.6; $p < 0.05$), while the freight increment did not change from the previous case.

2.4 Discussion

As displayed in Figure 2.4, our results indicate that the average change from passing coal trains adds approximately 8.3 µg/m^3 (95% CI = 6.4, 10.3) to the ambient $PM_{2.5}$, with a range of midpoint estimates, based on the sensitivity analysis, of 5 to 12 µg/m^3. These results suggest that full coal cars contribute approximately 2 to 3 µg/m^3 of $PM_{2.5}$ more than freight trains observed in our Richmond, California sample. Strikingly, with very calm winds, the nearby concentrations from coal trains were about 12 µg/m^3 versus 5.1 for freight trains. The contribution of coal cars increases to 25 µg/m^3 when we have calm winds from the west (n =3). This suggests the possibility of our study underestimating the emisssdions and overall impact of dust from coal trains, since, on windier days, the dust may be dispersed over a wider region beyond our monitoring site.

Figure 2.4 Alternative models of the change in $PM_{2.5}$ (5 min avg, µg/m3) from passing trains

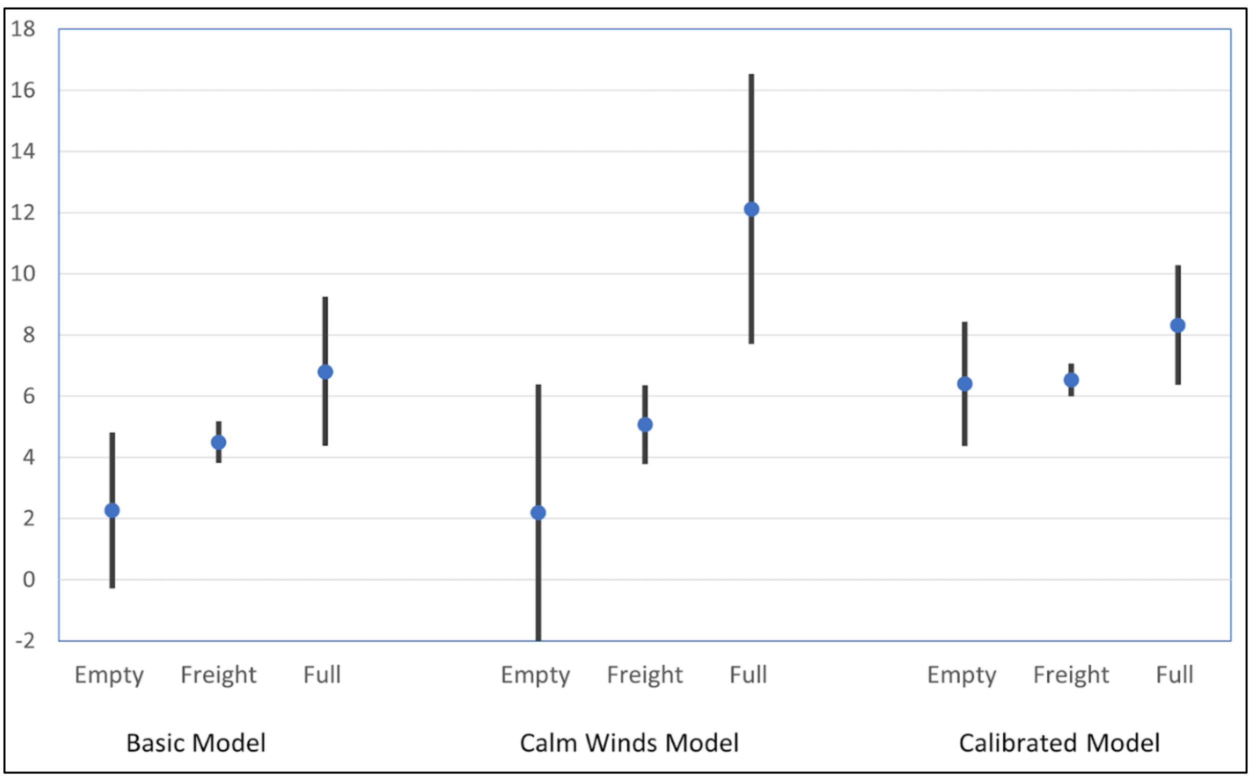

We also observed that unloaded coal cars tended to add 2 µg/m^3 of $PM_{2.5}$ to the existing ambient concentrations, with a range from our sensitivity analysis ranging from about one (non-significant) to over 5 µg/m^3.

Regarding peak (10-second) concentrations of $PM_{2.5}$, the calibrated model indicated an increase of 17.4 µg/m^3 (95% CI = 6.2, 28.5) from coal trains which tended to contribute about 3.5 µg/m^3

more than freight trains across the models examined. Calm wind conditions resulted in an increase from coal trains of 20 μg/m^3 (95% CI = 3.4, 36.6; p<0.01).

Given the known bias of humidity on optical PM monitors, in addition to controlling for humidity and dewpoint directly in the model specification, a regression model was estimated using data calibrated and corrected for humidity using a nearby FEM monitor (Barkjohn et al. 2021). It is well established that mass calibrations of optical sensors are temporally and spatially dependent on particle optical characteristics (Dubovik et al. 2002; Bond and Bergstrom 2006). The assumption is that consistent calibration factors from monitors within the same geographic region and time period are reasonable surrogates for in situ calibration.

Only a few previous studies have measured $PM_{2.5}$ concentrations from coal trains. One study examined coal and freight trains passing through the rural Columbia River Gorge (Washington) in the summer of 2014 (Jaffe et al. 2015). The study examined the difference between the 10-second maximum $PM_{2.5}$ and the background concentration. The authors observed a doubling in peak concentration for coal trains (20.9 μg/m^3) versus freight trains (10.7 μg/m^3). As illustrated in Figure 2.5, this is fairly consistent with our results for a similar averaging time of 17.4 μg/m^3. The average effective wind speeds in the Jaffe study were much higher than those in our study and were often associated with very high concentrations of $PM_{2.5}$. This suggests that $PM_{2.5}$ concentrations associated with train passage are likely to be even greater in certain areas farther away from the City of Richmond's urban setting due to greater train speeds.

A previous study collected data on coal trains operating in the Fraser River Delta area of British Columbia, Canada. In comparing ambient air impacts (one minute peak) of the coal trains (n = 20) to those of non-cola trains, the results suggested an increase of 5.3 (a 54% increase over background), 4.1, and 2.6 μg/m^3, respectively, for PM_3 (comparable to $PM_{2.5}$), PM_{10}, and PM_{20}, with occasional spikes in PM_3, from coal trains to 100 μg/m^3 (Akaoka et al. 2017).

Figure 2.5 Comparison of studies examining peak changes in $PM_{2.5}$ from passing coal cars

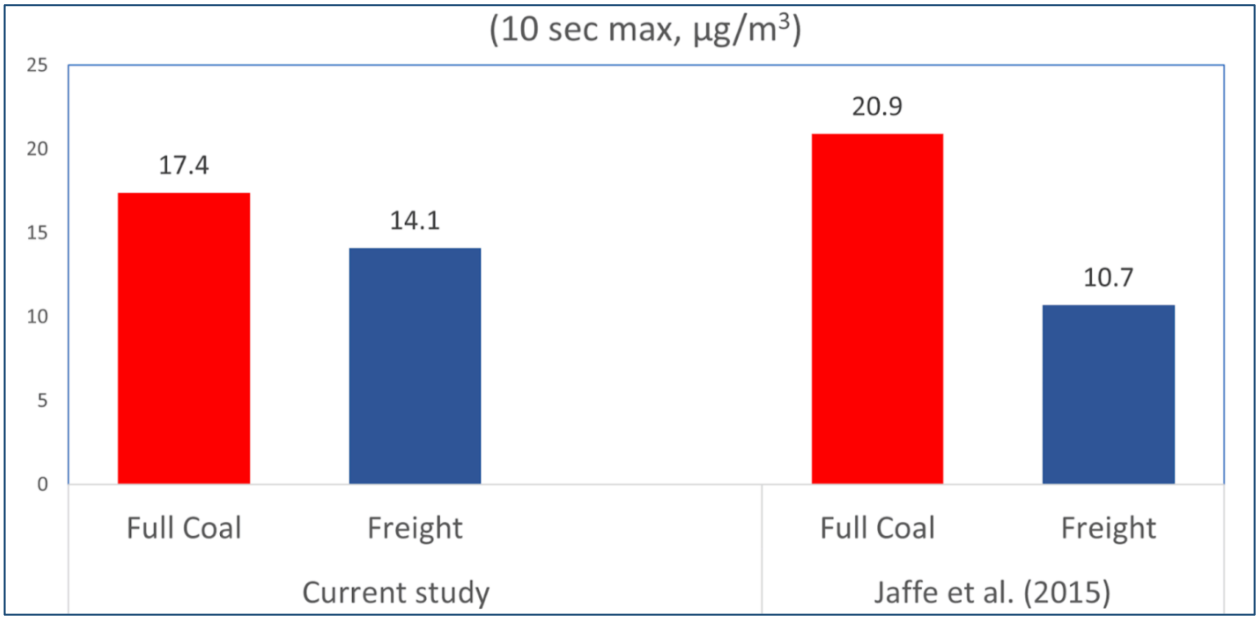

Another study collected data from four monitors located at varied distances from the train line on full (n = 36) and empty (n=33) coal trains heading to and from the Port of Newcastle in New South Wales, Australia (Higginbotham et al. 2013). For full coal cars, there were increases of 2.9 and 7.2 µg/m3, respectively, for $PM_{2.5}$ and PM_{10} and 7.1 and 18.9 for empty coal cars. Higher impacts for empty coal cars were also reported in studies by Katestone (2013).

Finally, Ryan and Ward (2014) analyzed the impacts of freight, empty coal, and full coal trains in the Hunter Valley in New South Wales, Australia (Ryan and Ward 2014). The crude (unadjusted) increases in $PM_{2.5}$ for passing freight, empty coal, and full coal cars were 0.53, 1.13, and 1.20 µg/m^3, respectively; all were statistically significant differences from baseline levels. Their measurements indicated that particulate level concentrations were elevated during, before, and especially after a train's passing. The range of findings from these studies is displayed in Figure 2.6.

Most of the dust from coal trains occurs from the rail car (80%), with spilled coal (9%) and door leakage (6%) being other sources (Connell Hatch 2008). A consequence is coal dust deposition, with studies finding that, on average, coal composed 6 - 25% of deposited dust in rail corridors, although Akaoka et al. report up to 90% in local dust (Akaoka et al. 2017; DSITIA 2015). Evidence indicates that particulate matter from coal trains, storage, and open mines can disperse at least 500 m from the source (Trevadi et al. 2009; Akaoka 2017; Srivastava et al. 2021; Sahu 2022).

For perspective, the current U.S.EPA annual and 24-hour average standards are 12 and 35 µg/m^3, respectively, while the World Health Organization guidelines for the same averaging times are 5

Figure 2.6 Comparative studies of increase in $PM_{2.5}$ Concentrations ($\mu g/m^3$)

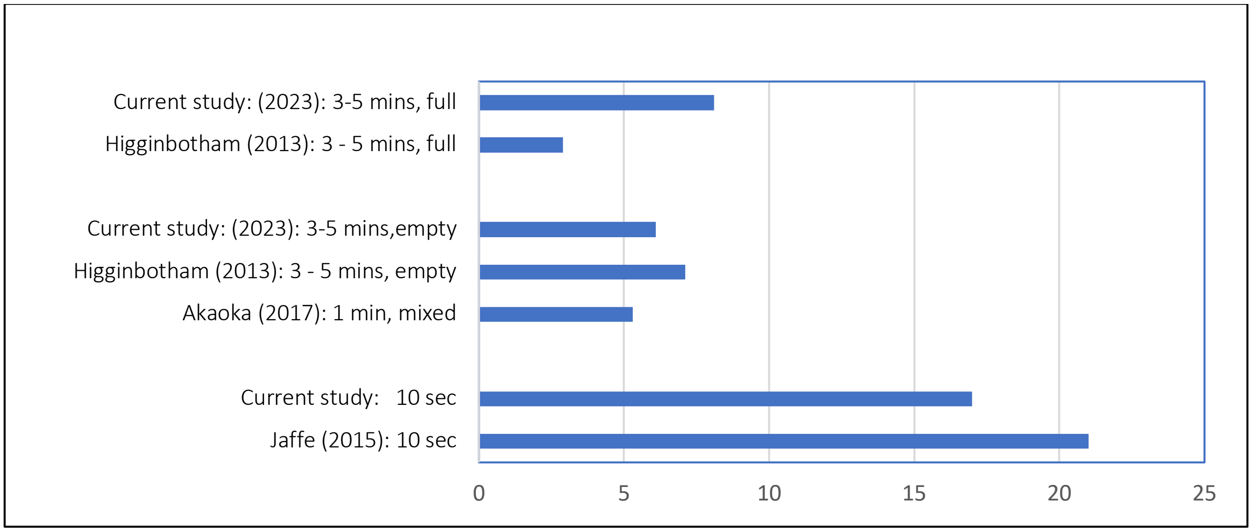

and 10 $\mu g/m^3$ (U.S. EPA, 2019; World Health Organization, 2021). In addition, both U.S. EPA and WHO indicate no threshold or safe level for ambient $PM_{2.5}$. Therefore, a hypothetical four to six coal trains per week in an urban area could represent an important increase in $PM_{2.5}$ to nearby residents. Incremental concentrations would subsequently increase the risk of a wide range of health effects, including premature mortality, cardiovascular and respiratory hospitalization or urgent care visits, increases in or exacerbation of asthma, adverse birth outcomes (e.g., low birth weight, prematurity, birth defects, and neurodevelopment), possible neurological impacts in children and adults (autism, Alzheimer's, Parkinson's) as well as impacts such as days with respiratory symptoms, restricted activity, and work or school loss (WHO 2021). As noted above, even acute $PM_{2.5}$ exposures as short as one hour (or a few hours) can increase the risk of adverse health outcomes, including acute myocardial infarction, hospitalization and emergency department visits for cardiovascular and respiratory disease, ambulance calls, and asthma exacerbation (Yorifuji et al. 2014; Kim et al. 2015; Chen et al. 2019).

Our study has several advantages, including the development of an AI-based platform for precise identification of train types during the day or night; real-time measurement of $PM_{2.5}$ and meteorology; siting of a monitor with only the trains as a source of $PM_{2.5}$; and the ability to produce data on train direction and speed. There were also some shortcomings in our study. The reduction in economic activity during the COVID-19 pandemic and related supply chain issues led to a relatively small number of full and unloaded coal cars. There was only a single monitor to measure the impact of passing trains. This was due to both logistical constraints pursuant to the COVID-19 pandemic and the difficulty in finding monitor host sites that were not impacted by other $PM_{2.5}$ pollution sources in Richmond, a city transected by major highways, refineries, other heavy industry and a port. There is the possibility of exposure misclassification if some of the freight trains also included coal cars.

The low R^2 in some of the models could be due to several factors, including the assignment of hourly wind, temperature, and humidity to the 4-5 minutes of train passage and uncertainty in estimating train speed and length. There were also unmeasured factors, such as train weight and number of engines. Finally, it is important to note that our analysis did not include measurements of either ultrafine (particles less than 0.1 microns) or coarse particles (PM10), which will always be generated from passing trains. Since there is substantial evidence of adverse health effects from both particle sizes, the actual health risks posed by passing coal trains are underestimated in this present study (Adar et al. 2014; Ostro et al. 2015).

Identifying the source of fugitive dust is important because the implications of exposure extend beyond individual and population health effects to matters of environmental and racial justice (Mikati 2018). While coal dust can have far-ranging population exposures, the communities in relatively close proximity to the rail lines will be disproportionately exposed. These residents are more likely to be of lower-income or people of color (or both) and also more vulnerable to adverse health outcomes (A. Hricko et al. 2014; Jha & Muller 2018).

Finally, the impacts of the rail transport of coal are compounding because it involves traversing thousands of kilometers, meaning multiple environmental justice communities are impacted. Ecosystems such as rivers and coastlines also receive extended exposure as the rails often trace their contours. Further, the climate change implications of coal transport, storage, and handling are significant, resulting in up to 16% of US carbon pollution (Meyer 2019).

2.5 Conclusion

In this section, we have reported evidence of significant increases in $PM_{2.5}$ due to passing coal-carrying trains in Richmond, California. The observed increases were greater than those produced by freight trains and passenger trains. Unloaded coal cars also generate increases in $PM_{2.5}$ at lower concentrations than full coal cars. Quantifying the contribution of coal trains in urban air populations is important since vulnerable communities are typically found close to rail lines. In addition, the inevitable dispersion of $PM_{2.5}$ will increase population exposure over a much wider area. Since the shipment of coal by train occurs worldwide and for many urban areas, it represents a significant public health hazard. Finally, to overcome technical challenges that have historically been barriers to the study of coal trains, we developed an artificial intelligence-driven monitoring platform to detect and quantify air pollution from passing trains. These advancements will contribute to future studies of health effects from mobile sources.

3. Coal-related $PM_{2.5}$ effects from holding yards

Coal trains often comprise 100 or more cars and can reach a mile in length. As a result, they exceed the processing capacity of the terminals that load and unload them and require additional industrial infrastructure, such as holding yards for both full and empty coal cars. Railcar holding sites may be found in several locations throughout a community, making them a potentially significant health hazard. In the City of Richmond, California, the main railyard is just under a mile east of the Terminal (see Figure 1). This site regularly stores both full or unloaded coal cars and full and unloaded freight trains. The trains will contribute to $PM_{2.5}$ increments not only from the diesel exhaust of train engines but also from fugitive coal dust. The latter likely contributes relatively more than diesel since cars often sit unmoved for hours or days.

However, a challenge to determining the independent contribution of coal trains to ambient $PM_{2.5}$ is the constant concomitant presence of freight cars in the holding yard. The present study attempts to overcome this barrier by collecting hourly $PM_{2.5}$ concentration data that recorded the train types at the rail yard. In this manner, we could compare periods with only freight trains versus periods with either full or unloaded coal cars located there. We provide additional characterization of $PM_{2.5}$ increases by examining various meteorological conditions and by graphical analysis.

3.1 Methods and Materials

3.1.1 Data collection

Hourly $PM_{2.5}$ data from the railyards were collected from May 27, 2021, through September 25, 2021, and from February 15, 2022, through October 27, 2022. Measurements were obtained from a monitor located approximately 700 feet ENE of the center of the holding area (Figure 1). There was a total of 200 days with observations. We utilized the same train detection methods described in Section 2 above, with four exceptions. First, still photographs rather than videos were taken of the railyard every minute for manual classification. Second, rather than the pre-event controls used in the passing train analysis, we used concurrent data from four purple air monitors that were approximately one mile SSE and generally upwind of the rail yard as controls (Figure 3.1). The hourly change in $PM_{2.5}$ was then calculated as the difference between $PM_{2.5}$ at the railyard and concentrations at these five monitors.

Both sets of monitors used the Plantower PMS5003 laser particle counter (as used in Purple Air monitors) and were corrected for humidity and calibrated using the same equation as in the passing train analysis. The third difference was the creation of hourly averages of $PM_{2.5}$ as opposed to the 4 - 5 minutes of the passing trains that were analyzed above. Finally, rather than a monitor proximate to the source as in the previous section on the passing trains, the monitor for the holding yard was located on a rooftop approximately 260 yards northeast of the center of the holding yard.

Figure 3.1 Holding yard with amplification and control sites

3.2 Analysis

Multiple linear regression was used to explain the variation in the change in $PM_{2.5}$. Since the hours when a full or unloaded coal train are observed are not all the same as the freight trains days, we controlled for factors that might change on a daily or hourly basis. Therefore, the basic model included terms for hourly temperature, wind speed and wind speed squared. The latter is necessary due to the apparent quadratic form of the $PM_{2.5}$ wind speed relationship as determined from sensitivity analysis. Sensitivity analysis also examined the impact of including other covariates in the model and impacts during windier hours and very calm hours. In addition, since there are some days with multiple observations, we examined the impact of fixed effect models, which control for the repeat measures.

3.3 Results

There were 4,670 hourly observations over 200 days of observations consisting of 1,097 full coal cars, 1,371 unloaded cars, and 2,102 freight cars. Table 3.1 displays the results of the regression analysis. In the basic model (Model 1), all three train types contributed to $PM_{2.5}$ increments at statistically significant levels ($p < 0.01$), with significant associations from the covariates temperature and wind speed. The $PM_{2.5}$ increase for full and empty coal was basically identical at 2.40 µg/m^3 (95% CI = 2.10, 2.69 ; $p < 0.01$). During the hours when only unloaded car cars were observed, the increment was approximately 0.25 µg/m^3 lower. All the estimates were statistically different from each other.

Table 3.1 Regression results of increase in $PM_{2.5}$ (µg/m3) for trains at rail yard

Model	(1) Basic	(2) WS>6	(3) WS>7	(4) FE	(5) FE WS>6	(6) FE WS>7	(7) FE WS<6
Full	2.40***	3.02***	2.76***	3.01***	2.74***	2.00***	3.54
Unloaded	2.16***	2.54***	2.21*	3.02***	2.76***	2.10*	3.64*
Freight	2.40***	2.90***	2.57***	2.85**	2.49***	1.87***	3.38***
n	4,571	2,282	1,695	4571	2,282	1,695	2,032
R^2	0.24	0.11	0.14	0.15	0.10	0.16	0.18

Note: ***$p < 0.001$; **$p < 0.01$; * $p < 0.05$; Basic = base model with WS, WS^2, temperature and the three train types; WS = Wind speed (m/s), FE = fixed effects model

Next, we examined the role of higher wind speeds through two subsets of data: one including only observations where wind speed was greater than the mean of 6 m/s (Model 2) and the other with wind speed greater than 7 m/s (Model 3). The results showed an increase in the difference in $PM_{2.5}$ between coal cars versus freight cars during the hours of higher winds. Specifically, at 6 and 7 m/s the statistically significant difference was 0.1 µg/m^3 and 0.21 µg/m^3, respectively.

Models 4 -7 replicated the above analysis using a regression model with fixed effects, which controls for multiple hourly observations on a given day. Model 4, which used a specification similar to the basic model, indicated a $PM_{2.5}$ increment of 3 µg/m^3 (95% CI = 2.05, 3.43; p<.0.01) for full coal cars with a similar estimate for empty coal cars. The estimates for empty and full coal cars were statistically higher than that of only freight cars by 0.16 μg/m^3. Model 5, which included only days greater than the mean wind speed of 6 m/s, showed a $PM_{2.5}$ increase of approximately 2.74 μg/m^3 for both full and unloaded coal cars, a statistically significant increase over freight trains of 0.25 μg/m^3.

Next, Model 6, which considered days with wind speed greater than 7 m/s, indicated a statistically significant increase of 0.13 μg/m^3 and 0.23 μg/m^3 for full and unloaded cars, respectively, over freight trains. Finally, Model 7 examined the $PM_{2.5}$ increases under calm wind conditions, with winds less than the mean of 6 m/s. Under these conditions, the unloaded trains demonstrated the largest increase in $PM_{2.5}$ at 3.64 μg/m^3 (95% CI = 3.19, 4.08; $p < 0.05$), which was 0.26 μg/m^3 higher than both full coal and freight trains.

It is enlightening to examine the graphs relating change in $PM_{2.5}$ to wind speed for each train type (Figure 3.2). Though scales are different, the graphs show that full coal car $PM_{2.5}$ changes are greater at the higher wind speeds from 7 to 13 m/s, unloaded cars have higher effects at lower wind speeds, and the increase for freight cars is enhanced at the 6 to 8 m/s wind speed.

Figure 3.2 Change in $PM_{2.5}$ and wind speed for three train types

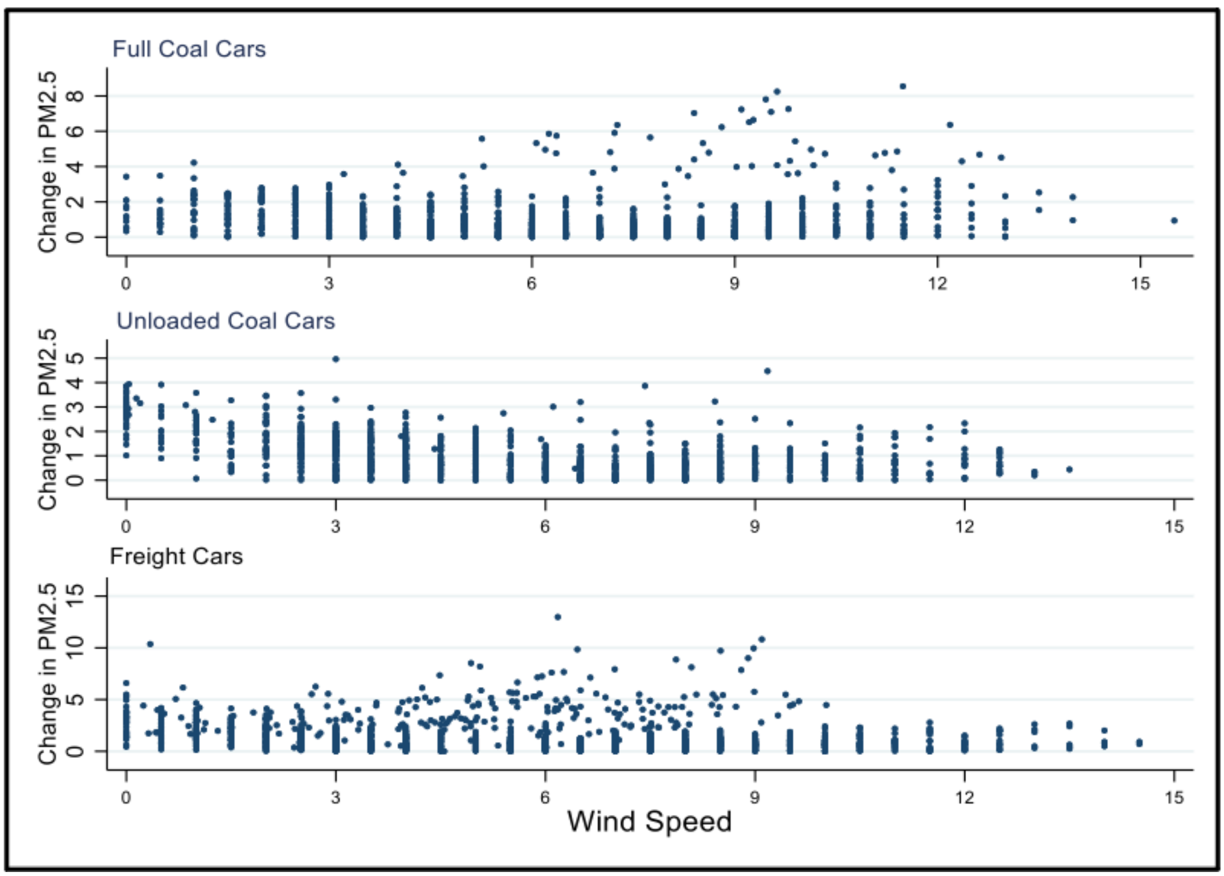

3.4 Discussion

All three train types kept at the train yard contribute to increments in $PM_{2.5}$, most likely via black carbon from diesel combustion resulting from relocating the trains in and out of the rail yard. However, our results using hourly data suggest an additional independent impact from fugitive coal dust from both full and empty (unloaded) coal cars, particularly during times of higher winds. The regression analysis suggests these cars could contribute 2 to 3 $\mu g/m^3$ of $PM_{2.5}$ above background concentrations. These $PM_{2.5}$ impacts are often 0.2 $\mu g/m^3$ greater than those of the diesel and dust contributions of freight trains. The diesel combustion contributes ultrafine particles (particles less than 0.1 microgram) that dominate particle numbers but not mass concentration (Schraufnagel 2020).

The results suggest that the contribution from full coal cars appears to significantly increase during windier days. In contrast, the contribution to ambient $PM_{2.5}$ from empty coal cars appears to be enhanced during days of relatively calm winds, a finding similar to that of Higginbotham et al. (2013). The difference in the contribution of full versus empty coal cars could be due to differences in the interplay between the location of the coal in the cars and their dispersion patterns relative to the monitor location. Specifically, high wind conditions may break through any surfactant or stacking barriers on full cars to release more dust because there is more coal in full cars. In addition, coal remnants in the unloaded trains are more likely to translocate than the full trains, and the coal may be drier, making them more susceptible to dispersion on lower wind speed days.

Some of these factors may also explain the modest R^2 observed in our regression models. Other explanations include the distance between the monitor and the middle of the holding yard; meteorology and other factors affecting the background monitors that might have differential impacts on the holding area; unmeasured covariates; and measurement error in the monitors even after calibration and correction. Finally, since $PM_{2.5}$ can remain in the air for hours and days, it's possible that there is some residual impact of emissions from prior hours traversing all the train types.

To our knowledge, very few studies have measured the impact of $PM_{2.5}$ from coal either at railyards or in urban areas in general, especially those that are highly populated. Jha and Muller (2018) reported a significant increase in $PM_{2.5}$ in a 25-mile radius around coal stockpiles stored at U.S. power plants. The analysis used the stored tonnage of coal at the power plant to predict $PM_{2.5}$, but there was no specific measurement of ambient coal concentrations. Tunno et al. (2018) observed multiple elemental and organic constituents of fine particles from coal in downtown Pittsburgh, including many known to cause adverse health effects.

While not specific to the impacts of holding yards, multiple studies of $PM_{2.5}$ concentrations and dispersion from open-cast coal mines suggest fugitive dust in urban settings will reach residential neighborhoods. For example, Sahu and Patra (2020) reported exposures related to coal mine operations in eastern India. The average $PM_{2.5}$ at the mine pit was 205 µg/m^3, which reduced to 151 µg/m^3 500 meters downwind, a 26% reduction indicating that the full dispersion range may be extensive. Trivedi et al. (2009) measured total suspended particulates (TSP, particles of any size) and utilized a dispersion model specific for fugitive dust at another open-cast coal mine in India. The authors report concentrations at the pit of around 350 µg/m^3, which dropped to still very high levels of about 100 µg/m^3 at a distance of 500 meters from the pit. It should be noted that due to its smaller size, $PM_{2.5}$ will travel much farther than total suspended particles (TSP).

Tecer et al. (2008) placed $PM_{2.5}$ monitors in the city center of a coal mining town in northwest Turkey and reported mean concentrations of 29.5 µg/m^3. The mines were 5 km west, 7 km south, and 12 km east of the city center. Finally, a study in southwest Virginia measured PM_{10} from trucks hauling coal along narrow roads from a nearby mine (Aneja et al. 2012). The two roadside monitors had averages of 138.5 µg/m^3 and 250.2 µg/m^3. There are also studies of the diesel impacts from train yards, but they do not include specific measurements of coal's contribution to ambient air (ARB 2008; Cahill 2011). These dispersion patterns are subject to changes in several factors, such as wind speed and humidity.

3.5 Conclusion

Since coal trains often comprise 100 or more cars and can reach a mile in length, extensive infrastructure, such as holding railyards or stockpiles, is required for storage as part of conveyance to and from export terminals or power plants. During this storage time, full and empty (unloaded) coal cars can emit $PM_{2.5}$ from diesel combustion and fugitive coal dust. The resultant $PM_{2.5}$ will result in exposures to populations near the rail line and, due to dispersion, to those residing further downwind. Given overwhelming evidence for the adverse health effects associated with $PM_{2.5}$, rail yards can represent an important health hazard for the community. Our study of such a railyard in the City of Richmond, CA, suggests that emptied and full coal cars can contribute 2 to 3 µg/m^3 of $PM_{2.5}$ above background concentrations. These measures are independent of the presence of freight cars, with wind speed leading to fluctuating concentrations. Other research suggests that this fugitive coal dust can travel extensively.

To isolate the contribution of coal, our study overcame several barriers. For example, we developed and utilized an AI-driven camera system to identify coal cars and control for freight train presence. We developed an integrated system that measured meteorological factors and real-time measures of fine particulate matter. The optical particulate measures were calibrated and corrected for humidity, following currently accepted methodology. Finally, we utilized multiple regression analysis to isolate the impact of specific train types. As such, our research is unique as we are unaware of any other studies that have specifically measured the coal component of $PM_{2.5}$ from holding yards. Fugitive dust is likely to reach surrounding residential communities, and neighborhoods near fossil fuel infrastructure are more likely to house people of color and low-income people. Therefore, the fugitive dust from coal cars in railyards represents an environmental justice concern and a health hazard.

4. Coal and petcoke effects from terminal operations

Despite improvements to facility designs and operations, coal particulates can persist even when piles are sprayed with water or a topping agent (Jha and Muller, 2018). Further, irregularities in terminal operations are common, even in well-designed settings, resulting in additional emissions (Higginbotham 2014). Therefore, it is likely that coal terminal operations lead to fugitive emissions that reach surrounding neighborhoods. To assess the potential impact on ambient air quality, specialized air monitoring instruments capable of identifying individual particles were deployed at multiple locations in and around the terminal area of Richmond. The complementary set of sampling and analysis methods utilized to identify coal and petcoke pollution are described below.

4.1 Specific particle identification of coal and petcoke methods and materials

To uniquely identify and quantify coal and petcoke particles in and around the Richmond terminal area, passive sampling of ambient particulate matter occurred during the summers of 2020 and 2022. Single particle analysis was then conducted using Computer Controlled Scanning Electron Microscopy (CCSEM) at the RJ Lee Group laboratories, an independent laboratory.

4.1.1 Reference material preparations

For the present study, reference materials of Wasatch Plateau coal and two forms of local refinery petcoke, one green and one calcined, were obtained by UC Davis to compare against the samples collected in the ambient environment. To prepare these materials for analysis, a portion of each was manually ground in a mortar and pestle, passed through a 20 µm sieve, and collected in a clean polypropylene test tube. All materials were cleaned with 70% ethanol and laboratory wipes until no visible residue was observed on the wipe. As a quality control measure to quantify any cross-contamination, consumer-grade sodium chloride samples were processed in the same way in between each reference sample. All reference and quality control samples were divided into two portions for analysis at the RJ Lee Group laboratory and UC Davis. No cross-contamination was observed in any of the sodium chloride samples.

4.1.2 Equipment

Ambient airborne particulates were collected at and surrounding the terminal using University of North Carolina Passive Aerosol Samplers (UNC-PAS) provided by RJ Lee Group (Wagner and Leith 2001b, c, a). The UNC-PAS samplers are considered “passive” in that they allow particles to settle on an adhesive carbon tab mounted on 13 mm SEM stubs according to general ambient conditions (in contrast to “active” monitors such as PurpleAir that use a fan to draw in air). To avoid deposition of large particles or biological contaminants (e.g., insects), they employ a wire mesh cap over the adhesive tab. A diagram of the sampling assembly is presented below in Figure 4.1. Figure 4.2 shows a deployed UNC-PAS with the protective housing (Ott and Peters 2008) at one of the monitoring locations.

Figure 4.1 Diagram of the UNC-PAS ambient particle sampling assembly

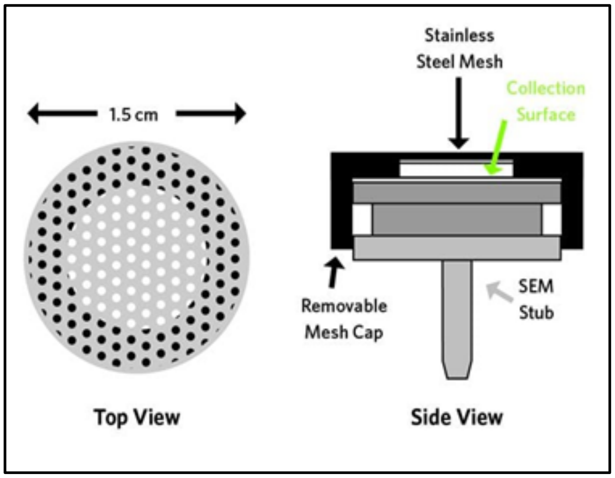

Source: RJ Lee Group, https://www.rjlg.com/unc-passive-aerosol-sampler/

Figure 4.2 Photograph of UNC-PAS sampler deployed at a terminal monitoring site co-located with a DRUM sampler*

The UNC-PAS is outlined in red. The photograph was taken facing south; the terminal facility is located to the southwest of this site

4.1.3 Ambient sample collection

All sampler deployments were documented on chain-of-custody forms provided by RJ Lee Group and photographed. A set of two samplers was collected between June 24th and July 9th, 2020 with a follow-up deployment consisting of five samplers between June 13th and July 18th, 2022. The initial deployment was deemed non-representative of normal human activities due to the COVID-19 pandemic shutdown. The second deployment in 2022 included five locations roughly aligned with a north-south orientation, including one upwind site located on Point Potrero and two downwind sites in the Santa Fe neighborhood northeast of Levin Terminal. The 2022 monitoring locations are presented in Figure 4.3.

Figure 4.3 UNC-PAS monitoring locations for the 2022 deployment

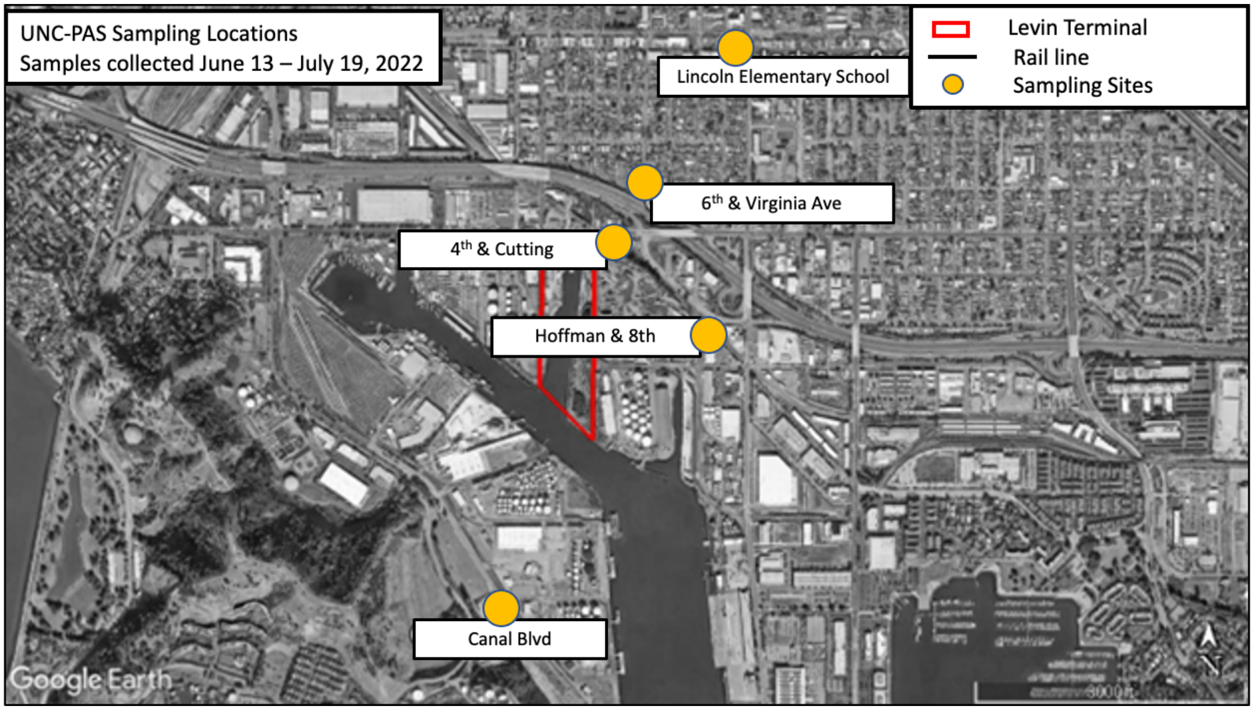

The Levin Terminal is outlined in red while the monitoring sites are identified with orange circles and labeled with their cross streets.

To increase the geographic reach of particle collection, additional samples were collected via adhesive carbon strips (tape). Surface particles were collected from street signs, light poles, and park fencing throughout the study area on October 20, 2022. Particles on the carbon strips were then placed in clean Petri slides and labeled. This form of surface sampling is easily obtainable and can increase the number of sampling sites for better spatial coverage. Since the results of this analysis were only used to identify the presence of coal and petcoke particles, regardless of time or other conditions, the surface sample collection was an appropriate adjunct approach, even as surface samples have no temporal representation and are impacted by uncontrollable factors including precipitation and hyper-local sources. These samples were assessed at UC Davis using a Thermo Fisher Quattro S SEM in the Advanced Materials Characterization and Testing facilities (https://mse.engineering.ucdavis.edu/amcat/thermo-fisher-quattro-s).

4.1.4 Sample analysis overview

Samples from the UNC-PAS samplers, along with the reference materials, were analyzed by Computer Controlled Scanning Electron Microscopy (CCSEM) at the RJ Lee Group laboratories. Their documented methodology (Casuccio et al. 1983) can be summarized in four main steps: particle detection, micro-imaging, particle measurements, and chemical characterization. A graphical summary is shown in Figure 4.4. The particle detection step, or prospecting, employs

Figure 4.4 A graphical representation of the IntelliSEM particle analysis

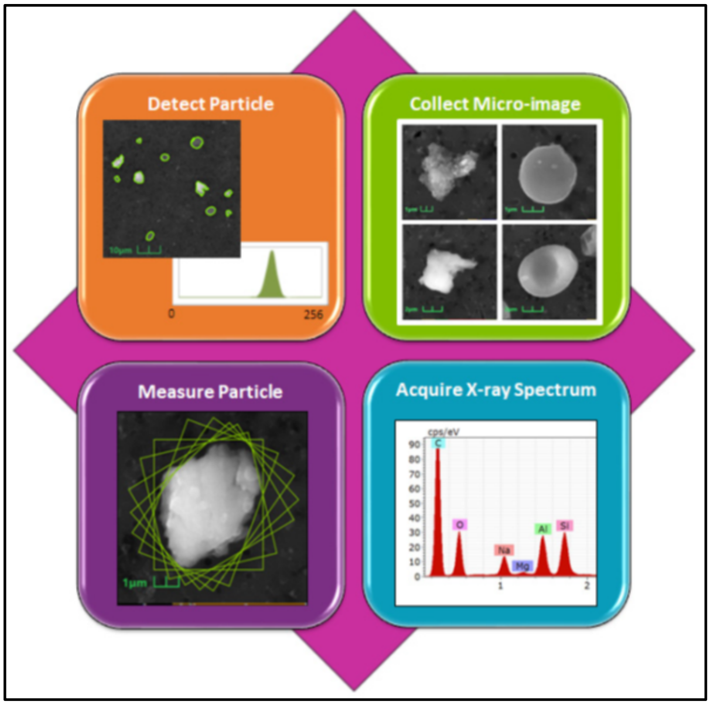

The process consists of 1) Detect Particle, 2) Collect Micro-image, 3) Measure Particle, and 4) Acquire X-ray Spectrum. The images shown in this graphic are not from samples collected during this study

an automated algorithm to detect individual particles on a sample substrate. The particles' size, shape, and chemical composition produce more backscattered electrons (BSE) than the carbon substrate, thus enabling distinction by analyzing the BSE detector pixel intensity distribution. Once particles and their locations on the sample substrate are identified, the software selects a random sampling of 1,000 particles for further analysis. Each identified particle is imaged (micro-imaging) and then measured using 45 rotating Feret boxes, which result in 90 diameter measurements for each particle. The particle shape characteristics (e.g., aspect ratio, roundness, and elongation) can be accurately assessed by measuring diameters at many angles. For example, many biological spores are spherical, while crustal particulates are angular. The final step for each particle is semi-quantitative chemical speciation using energy dispersive spectroscopy (EDS). The EDS system acquires an X-ray spectrum from the particle and automatically associates it with the micro-image and dimensional measurements.

4.1.4 Sample analysis

Study samples were analyzed using RJ Lee's automated instrument control and analysis software (IntelliSEM) followed by RJ Lee personnel's manual inspection and quality assurance (Casuccio et al. 1983; Shen et al. 2016). Reference materials were deposited onto carbon tape for CCSEM analysis by RJ Lee and deposited on lightly greased Mylar for ion beam analysis at Crocker Nuclear Lab (see Appendices for details).

4.1.5 Quality assurance - quality control

The speciation analysis was predicated on the accurate determination of elemental concentrations. To determine accuracy, an inter-laboratory comparison of reference materials was performed between the RJ Lee CCSEM analysis and UC Davis ion beam analysis (IBA). Briefly, IBA is the detection of elemental concentrations using a beam of protons. This beam is generated by a particle accelerator, such as Crocker Nuclear Lab's cyclotron at UC Davis. (More details are provided in Appendix 3). The results of this comparison are shown by a scatterplot (Figure 4.5).

Figure 4.5 Inter-laboratory measurement technique comparison of reference material elemental compositions

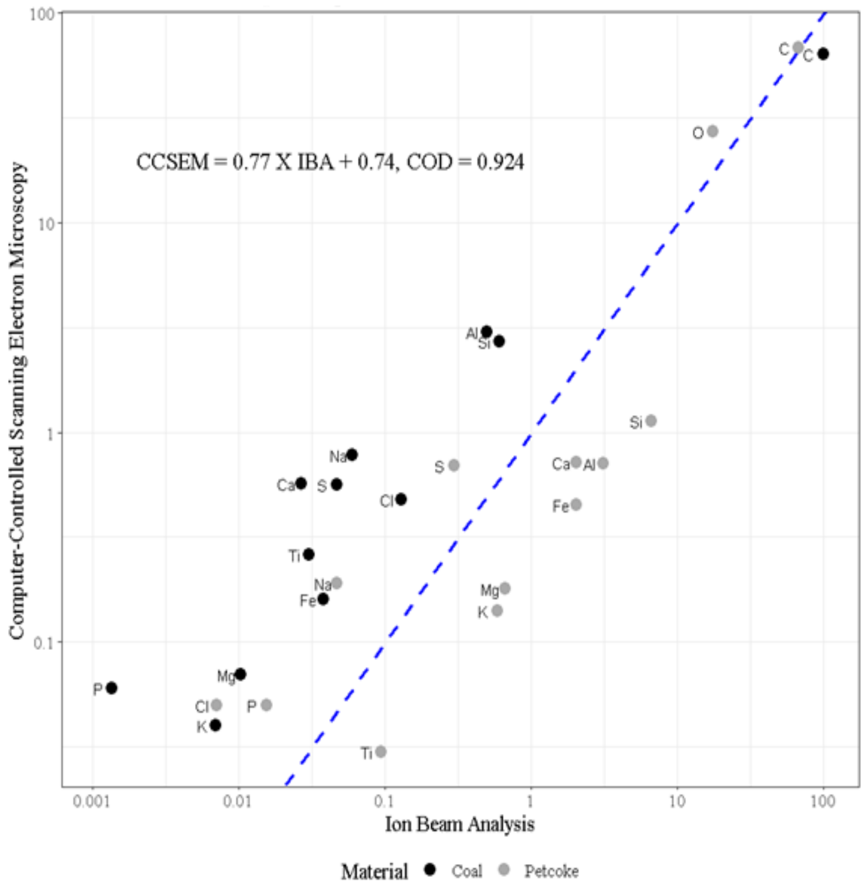

All values are in ng/m^3. The equation is derived from ordinary least squares regression while the dashed line represents 1:1 agreement. The closer the points are to the dashed line, the better the two methods agree.

The two reference materials, coal and petcoke, are shown as black and gray points, respectively. Perfect agreement between the two methods would show all points along the dashed line; however, there are always differences between measurement results due to the different strengths and weaknesses of each instrument (systematic error) and instrument noise (random error). Agreement from this direct comparison can be assessed using the slope and coefficient of determination (r2), both approaching one with better agreement. The closer the points are to the dashed line, the better the two methods agree. For example, carbon and oxygen measurements from both labs were very similar and the points lie close to the dashed line. On the other hand, the phosphorus of the coal sample measures much higher by CCSEM than IBA and thus lies far to the left of the dashed line. When multiple independent measurements provide the same or similar results, there is more confidence in their interpretation.

Differences may be due to sample loading effects in the IBA. The two methods generally agreed with a high coefficient of determination (0.92) and a slope of 0.77 using ordinary least squares regression. Although the CCSEM generally measured higher concentrations for the coal sample and lower concentrations in the petcoke sample than ion beam analysis, the difference was not substantive because the identification of coal and petcoke used elemental ratios (relative relationships) rather than absolute concentrations. The ratios of coal and petcoke related elements were conserved for both methods, meaning both the CCSEM and IBA showed similar chemical fingerprinting for the coal and petcoke and the CCSEM method was reliable for the identification of ambient samples.

The reference material coal particles were predominantly carbonaceous with inclusions of crustal elements silicon, aluminum, sulfur, and sodium chloride. Trace amounts of calcium, titanium, and iron were also detected. The two petcoke reference materials, green and calcined, presented different chemical and morphological signatures. The calcined petcoke sample was predominantly carbonaceous with fewer silicon, aluminum, and sulfur. Its trace constituents included particles of calcium-iron-magnesium, aluminosilicates, and silicon dioxide and showed higher calcium concentrations than coal and green petcoke. The green petcoke sample was distinctly glassy and angular, with higher sulfur content and fewer trace elements except silicon.

Although different relative abundances of trace elements were observed on manual inspection of particles, the chemistry and angular morphology of the coal and petcoke samples were too similar for statistical separation. Therefore, the following discussion will focus on the combined results of coal and petcoke particles.

4.2 Results from Specific Particle Analysis

Coal and petcoke particles were detected at the terminal and surrounding neighborhoods. They were specifically identified and differentiated from other carbon-rich particles, such as diesel, by their morphology (angular particle shapes) and chemical composition. Specifically, diesel and coal/petcoke particles were differentiated by 1) size, as coal particles were large, greater than 1 µm in most cases, while diesel particles are small, around 0.2 µm; 2) composition, as coal/petcoke particles naturally include crustal inclusions while diesel particles do not; and 3) morphology, as coal particles are more angular with edges while diesel particles are spherical. Figure 4.6 presents an image of coal particles from the reference material alongside diesel particles analyzed by Lee et al. (2021), with size a clearly distinguishing feature. *Note that the scale bars are 20 µm for the coal particles and 1 µm for the diesel particles.*

Figure 4.6 SEM micro-images of coal particles collected during this study (a) alongside diesel particulate matter (b) analyzed by Lee et. al. 2021 showing the size difference.

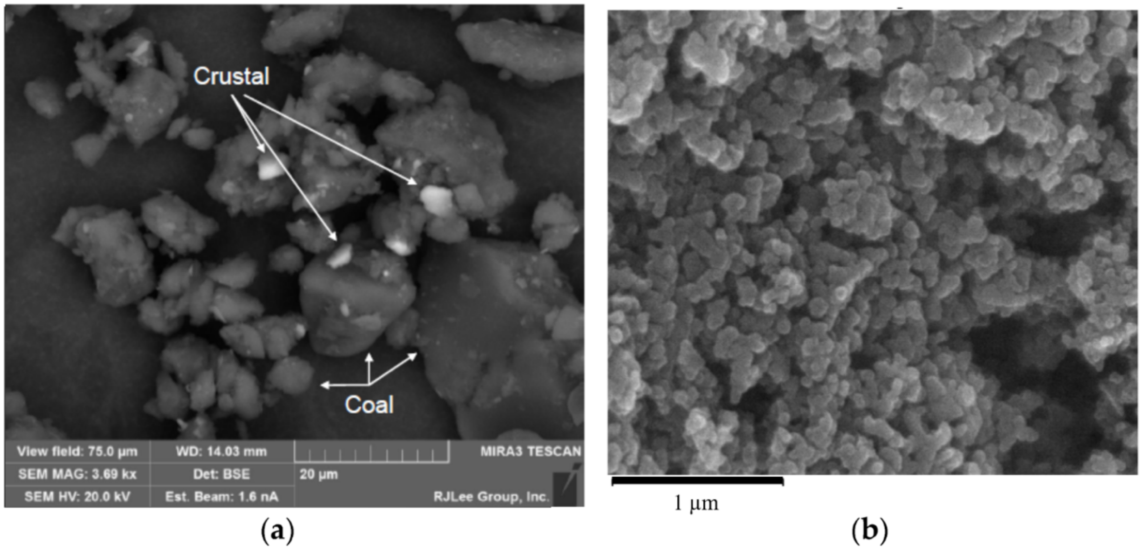

Figure 4.7 shows boxplots (statistical summaries) of the coal/petcoke particle diameters detected at the five monitoring locations in Richmond. The particle diameters were nearly all above 1 µm while diesel is found below 0.2 µm. The size range of diesel particulate matter is highlighted to underscore its size difference compared to coal/petcoke. Too few particles were identified at Harbour & Ohio for statistical summary, so its average diameter is shown as a horizontal line.

Figure 4.7 Coal and petcoke particle sizes (diameters) observed at each site.

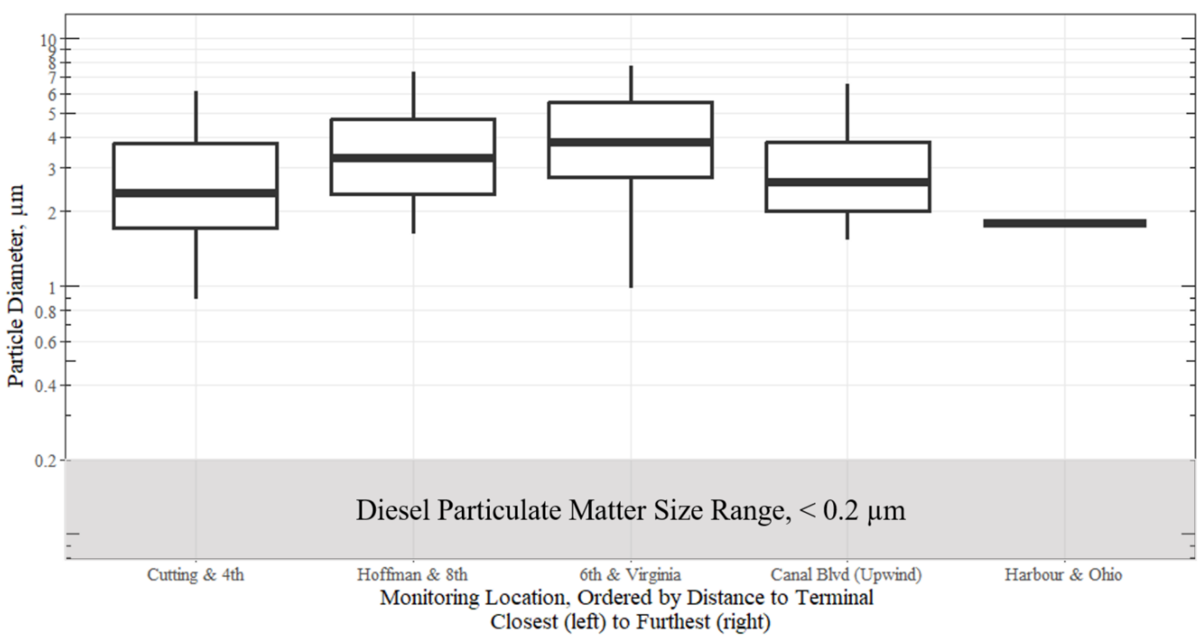

Fine particle concentrations of coal and petcoke ranging from 0.1 to 0.6 µg/m^3 were detected at all five monitoring locations. The identification of coal/petcoke in the ambient UNC-PAS samples is summarized by a map generated by RJ Lee and shown in Figure 4.8. The highest respirable ($PM_{2.5}$) concentrations are observed on either side of the terminal, with lower but still detectable concentrations extending to the nearby residential area.

Figure 4.8 Map of measured coal and petcoke $PM_{2.5}$ particle concentrations (µg/m^3) from the UNC-PAS samples.

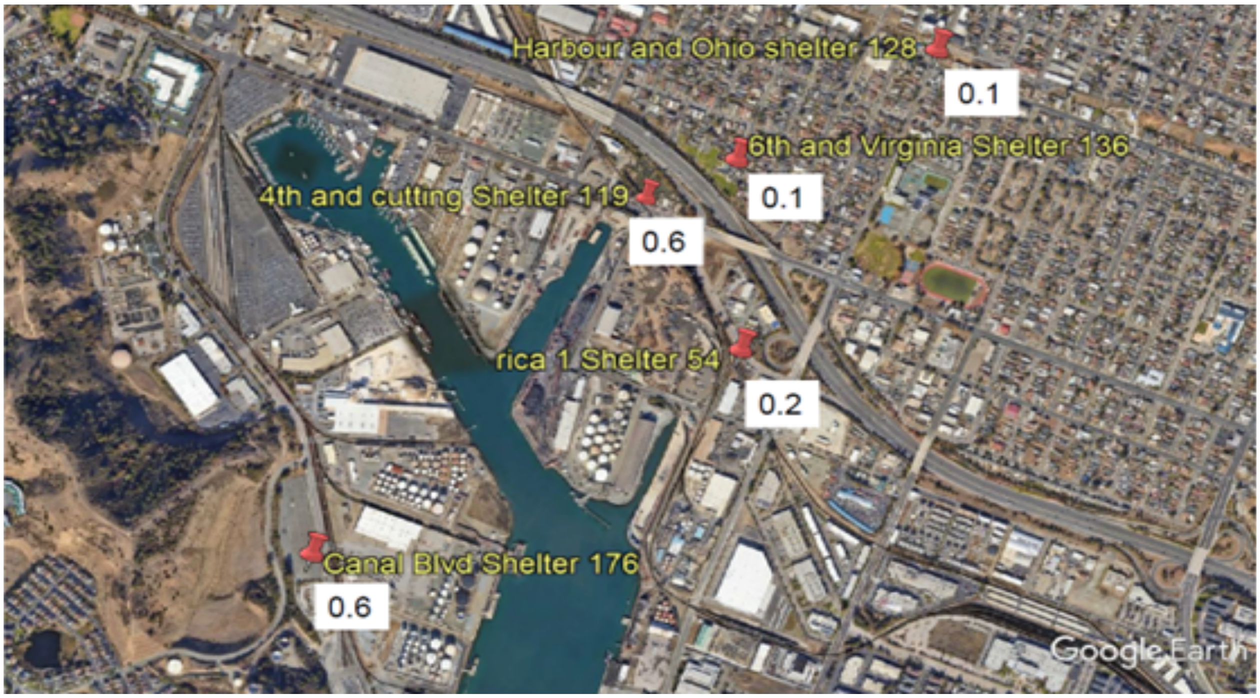

The CCSEM analysis also measured coarse particles, or particles with diameters between 2.5 and 10 micrometers ($PM_{10\text{-}2.5}$), which are known to have independent health effects. Not surprisingly, most of the coarse particle mass was from sea salt and crustal (soil) material. Nevertheless, coal and petcoke were still detected in this size range and are shown in Figure 4.9. Specifically, coarse particles were highest at the marine terminal (ranging from 0.4 µg/m^3 to 0.6 µg/m^3) and were lower at the furthest locations (< 0.1 µg/m^3 to 0.2 µg/m^3). This is consistent with expectations of larger particles settling closer to their source than fine particles, in this case terminal operations.

Figure 4.9 Map of measured coal and petcoke $PM_{10-2.5}$ particle concentrations (µg/m^3) from the UNC-PAS samples.

Additionally, very large (> 20 µm) coal particles were observed using manual SEM analysis by RJ Lee. Approximately half of these particles were observed close to the terminal at the 4th and Cuttings Ave monitoring location, providing additional confirmation that terminal operations are a source of fugitive coal dust. The remaining of these coal particles were more widely scattered in the surrounding neighborhoods.

These findings of coal/petcoke in the community are corroborated by analysis of surface (tape) samples. Carbonaceous particles matching the morphological and chemical characteristics of coal/petcoke were observed in the surrounding community, including near the Union Pacific rail line (Parchester Village, coal only) and several locations downwind of the Levin Terminal (Figure 10). Most of the observed particles from this analysis were large (> 20 µm). While a comprehensive and systematic sampling of particles was not performed on these samples, particles in smaller size mode are nevertheless likely to be present. Figure 4.10 shows the study area with inset micro-images of carbonaceous particles identified as coal/petcoke based on comparison with reference materials. The Levin Terminal is outlined in red, the rail car holding yard is outlined in green, and rail lines are shown as solid black lines.

Figure 4.10 Coal and petcoke particulate matter identified at the terminal and in the neighborhood

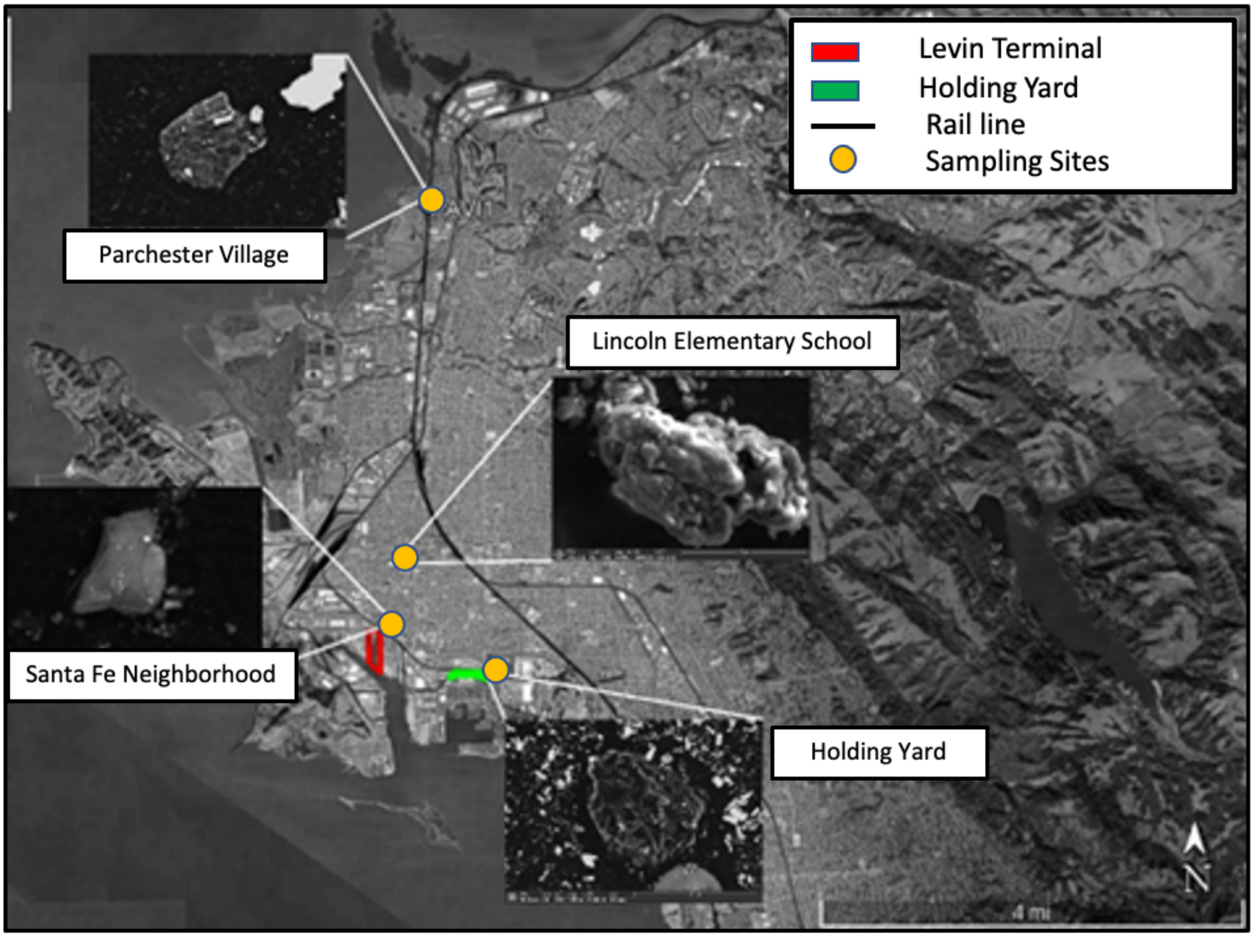

The CCSEM analysis confirms the presence of coal and petcoke at the terminal and surrounding neighborhoods. Further corroboration was provided by sampling and analysis using independent methods, namely DRUM (Davis Rotating Unit for Monitoring) sampling and IBA (detailed in Appendix 3). In brief, DRUM samplers collect particulate matter in eight discrete particle size bins at three-hour time resolution. The samples are analyzed for mass concentrations, optical properties, and elemental species in the UC Davis laboratory using several non-destructive methods, including IBA.

The primary supporting evidence this additional DRUM analysis provides is the form of elevated carbon/oxygen ratios detected upwind of the terminal. While carbon is ubiquitous, a high carbon/oxygen ratio measured by IBA (i.e., under vacuum) indicates that the carbon is in the solid, graphitic form seen with inorganic matter such as coal and petcoke instead of diesel or gasoline emissions. Figure 4.11 illustrates that the highest ratios (in yellow) come from the south, where the terminal is located. In contrast, the lower ratios (darker) are blowing in from the northwest along the highway.

Figure 4.11 Polarplot of carbon/oxygen ratios for all particle size bins measured at the terminal monitoring location.

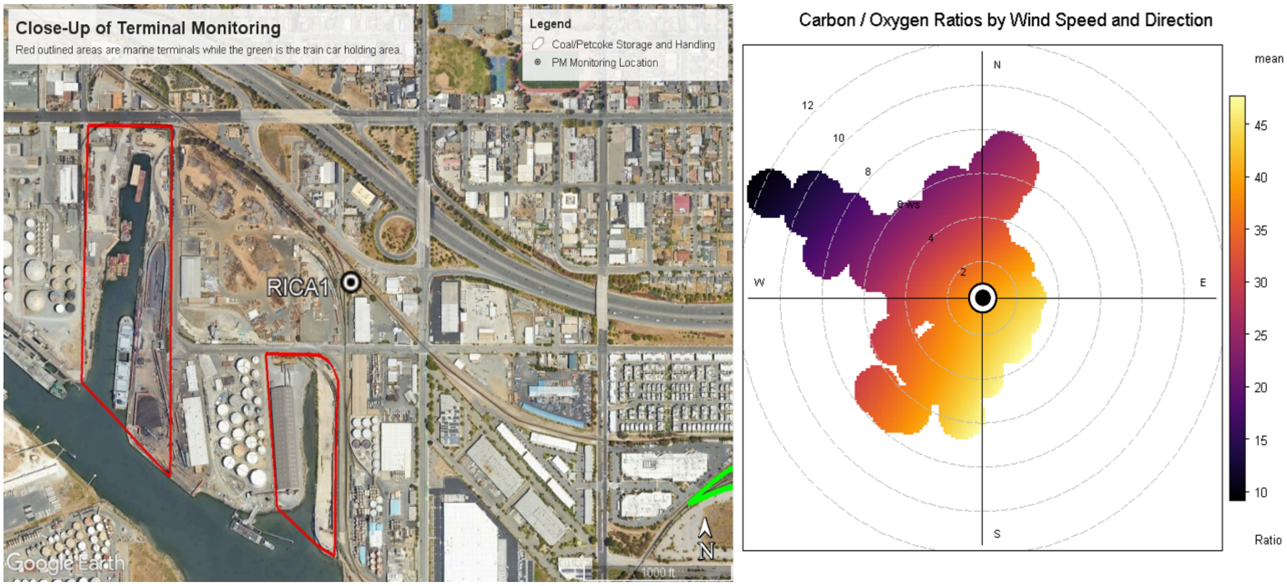

4.5 Conclusion

Coal and petcoke were definitively identified at the terminal and in residential neighborhoods using three independent methods: passive monitoring, surface tape sampling, and active DRUM monitoring. Concentrations ranged from 0.1 to 0.6 μg/m^3. Both coarse and fine coal particles were identified using separate independent laboratories and methods. These corroborative findings signal high confidence in the results. It is therefore reasonable to expect subsequent health effects due to coal and petcoke from terminal operations.

5. Health & environmental justice

Myriad large epidemiological studies definitively establish that exposure to $PM_{2.5}$ is associated with a wide range of adverse health effects. Exposure to $PM_{2.5}$ has been linked to premature mortality, cardiovascular, cerebrovascular, and respiratory diseases, other chronic diseases, adverse birth outcomes, and cognitive and developmental impairments (WHO 2021; EPA 2019). This impact holds even at concentrations lower than current regulatory standards (Brunekreef et al. 2021; Pinault et al. 2016) and at exposures as short as one hour (Bhaskaran et al. 2011; Liu et al. 2021; Peters et al. 2001; Wu et al. 2020). The World Health Organization recently lowered its threshold guidelines and indicated no known safe level of $PM_{2.5}$ (U.S. EPA 2019; World Health Organization 2021). The recent Global Burden of Disease study estimates that exposure to $PM_{2.5}$ contributed to 6.7 million deaths annually worldwide, nearly 12% of the global total and the fourth highest risk factor for global mortality ((McDuffie et al. 2021; Shea et al. 2020).

5.1 Public Health

Studies on the health effects of $PM_{2.5}$ have been conducted on 6 continents. The overwhelming consensus is a causal association between exposure to $PM_{2.5}$ and a wide range of health outcomes. The health effects range from mild respiratory irritation to premature mortality, and the exposure periods of concern range from hours to multiple years (WHO 2021; EPA 2019). These effects occur even at concentrations lower than current regulatory standards (Di et al. 2017; Pappin et al. 2019; Crouse et al. 2020).

The impacts of coal dust have traditionally been studied in terms of occupational exposure. Still, there is ample evidence to infer significant impacts for the general population from short and long-term ambient exposure to coal dust. While there is some evidence that the different components of $PM_{2.5}$, such as combustion-based particles (e.g., sulfates and elemental carbon) might be more toxic than other components, there is still uncertainty about the relative toxicity of the components (Thurston et al. 2021). Pending further evidence to the contrary, the Gates Foundation-funded Global Burden of Disease, conducted by the Institute for Health Metrics and Evaluation (IHME) located at the University of Washington, and many other studies of the disease burden from exposure to $PM_{2.5}$ have typically treated all particles as equally toxic (Lelieveld et al. 2015; Fuller et al. 2022). In addition, a recent World Bank review of the impacts of dust indicates there is sufficient evidence to raise concerns for public health (Ostro et al. 2021). The recent Global Burden of Disease study estimates that exposure to $PM_{2.5}$ contributed to 6.7 million deaths yearly worldwide, nearly 12% of the global total and the fourth-highest risk factor for global mortality (HEI 2020).

Below, we provide a brief review of some of the potential implications of exposure to coal-related $PM_{2.5}$ from immediate (an hour to multi-hours), acute (days to multi-days) to chronic (annual to multi-year) exposures. Full quantification of health impacts specific to the coal-specific $PM_{2.5}$ increments we measured is beyond the present study's scope since they depend on the continued development of appropriate dispersion models.

5.1.1 Exposure: Dispersion

While there is little empirical evidence specifically measuring the dispersion of fugitive coal dust from conveyance, storage, and handling, there is evidence from other sources that this dust will disperse far from the original emissions and into the community at-large. For example, Tunno et al. (2018) observed multiple elemental and organic constituents of fine particles from coal in the downtown Pittsburgh area, including many known to cause adverse health effects. Sahu and Patra (2020) reported exposures related to coal mine operations in eastern India. The average $PM_{2.5}$ at the mine pit was 205 $\mu g/m^3$ which reduced to a still high 151 $\mu g/m^3$ at 500 meters downwind, a 26% reduction indicating that the full dispersion range may be extensive.

Trivedi et al. (2009) measured total suspended particulates (TSP, particles of any size) and utilized a dispersion model specific for fugitive dust at another open-cast coal mine in India. The authors report concentrations at the pit of around 350 $\mu g/m^3$, which dropped to about 100 $\mu g/m^3$ at a distance of 500 meters from the pit. It should be noted that due to its smaller size, $PM_{2.5}$ will travel much farther than TSP. Tecer et al. (2008) placed $PM_{2.5}$ monitors in the city center of a coal mining town in northwest Turkey and reported mean concentrations of 29.5 $\mu g/m^3$. Finally, a study in southwest Virginia measured PM_{10} from trucks hauling coal along narrow roads from a nearby mine (Aneja et al. 2012). The two roadside monitors had averages of 138.5 $\mu g/m^3$ and 250.2 $\mu g/m^3$.

A full quantification of health impacts associated with coal-specific $PM_{2.5}$ is beyond the scope of the present study, pending development of relevant emissions factors and dispersion models. We are currently working with other researchers on this issue and hope to quantify health impacts. It is nevertheless still of community benefit to review below the likely health outcomes associated with $PM_{2.5}$ and describe the population potentially at risk.

5.1.2 Potential health effects

To date, most studies of $PM_{2.5}$ have examined the impacts of either acute (day or multi-day) or chronic (annual or multi-year) exposure periods. Epidemiologic studies have documented associations of $PM_{2.5}$ with an extensive range of outcomes, and new outcomes are continually being reported. In addition, the biological mechanism underlying these adverse effects have been confirmed in toxicological studies. As a result, many of these studies have been used to quantify the impact on local or global populations (Fuller et al., 2022). These studies include the following outcomes: premature mortality from all causes, cardiovascular and respiratory diseases; infant mortality; life expectancy; myocardial infarction; cerebrovascular diseases; diabetes; hospitalization for cardiovascular or respiratory disease; emergency room visits; asthma induction and exacerbation; adverse birth outcomes including low birth weight, prematurity, and birth defects; neurodevelopmental effects; cognitive impacts on adults (dementia, Parkinson's, Alzheimer's) and children (ADHD, autism, IQ); work and school loss and restrictions in activity (WHO 2021). In addition, many studies have reported associations with lung cancer and, more recently, several other organs.

Many of these studies have reported impacts at very low concentrations of $PM_{2.5}$ with no evidence for a threshold (i.e., no-effects) level (Pappin et al. 2019; Crouse et al. 2020). Such findings have driven the World Health Organization to recently lower their air quality guidelines for acute and chronic exposure (WHO 2021). While most of these studies use exposure windows of days to years, several studies have found impacts associated with very acute exposures of one or more hours. These studies might have particular relevance for the short $PM_{2.5}$ exposures from passing trains, although the particles may remain in the air for hours to weeks, thus constituting a source of chronic exposure as well. These studies indicate that these very acute exposures can increase the risk of adverse health outcomes, including acute myocardial infarction, emergency department visits for cardiovascular and respiratory disease, ambulance calls, and asthma exacerbation (Peters et al. 2001; Bhaskaran et al. 2011; Yorifuji et al. 2014, 2015; Kim et al. 2015; Chen et al. 2019; Chen et al. 2020; Wu et al. 2020; Liu et al. 2021; Fu et al. 2023).

In addition to increases in $PM_{2.5}$ from the transport and storage of coal, Section 4 findings also indicate significant increases in coal-related coarse particles (particulate matter between 2.5 and 10 microns in diameter) in the community. There are hundreds of studies reporting serious effects from exposure to coarse particles. These studies include effects on all-cause, cardiovascular, and respiratory mortality and morbidity impacts, including hospitalization for cardiovascular and respiratory disease and exacerbation of asthma (Adar et al. 2014; Chen et al. 2015; Chen et al. 2019; Davis et al. 2020; Nirel et al. 2018). In addition, a recent study of 205 cities across the globe reported important associations between coarse particles and premature mortality (Liu et al., 2022).

Several studies have specifically examined the impact of dust particles, as summarized by Ostro et al. (2021). Many of these studies focus on the impacts of blowing desert dust from the Sahara, Central Asia, and Australia and report significant cardiovascular and respiratory effects (Zhang et al. 2016; Aghababaeian et al. 2021). There are also studies that use daily data and report $PM_{2.5}$ effects associated with urban re-entrained dust, crustal material, or their tracer chemicals such as silicon and calcium rather than $PM_{2.5}$ directly. For example, Ostro et al. (2007) used daily data from 2000 to 2003 in eight metropolitan areas in California and reported associations between all-cause mortality and two markers of soil, calcium and silicon. Using time-series analysis of several years of daily data from Philadelphia, Sacks et al. (2012) reported associations between crustal material and cardiovascular mortality. Krall et al. (2013) used U.S. EPA Chemical Speciation Network data from 72 urban U.S. communities to indicate that several components, including silicon were associated with increases in mortality.

Dai et al. (2014) examined $PM_{2.5}$ data from 75 mostly Eastern and Midwestern U.S. cities and reported associations between the silicon constituent and both all-cause and cardiovascular mortality. Finally, Ostro et al. (2016) used $PM_{2.5}$ mass source apportionment data from eight major metropolitan areas in California and reported associations between emergency department visits for cardiovascular and respiratory diseases and exposure to soil. The study also found associations between soil and exacerbation of asthma. Taken together, the studies of daily exposures to dust or dust-like particles or their tracers provide reasonably strong support for an association with all-cause and cardiovascular mortality and, in some cases, respiratory mortality.

Besides the above studies that used daily measures of exposure, several studies examined chronic (multi-year) exposures to dust and its markers (e.g., silicon). For example, Ostro et al. (2011) examined long-term exposure to $PM_{2.5}$ components among 102,000 California women teachers and administrators from the California Teachers Study. Statistically significant associations were observed between cardiopulmonary mortality and the silicon component of $PM_{2.5}$. Vedal et al. (2013) used data from the Women's Health Initiative–Observational Study, a cohort of about 90,000 women from 45 U.S. cities across the nation, to investigate the effects of chronic exposure to $PM_{2.5}$ constituents and sources on cardiovascular mortality. Silicon was associated with deaths diagnosed as resulting from possible coronary heart disease. Thurston et al. (2013) examined the effect of $PM_{2.5}$ components and sources using data from the national American Cancer Society's Cancer Prevention Study-II cohort. Several constituents of $PM_{2.5}$, including soil tracers, calcium and silicon, were examined, and associations with both tracers were associated with respiratory mortality and ischemic heart disease mortality, including heart attacks. Crouse et al. (2016) utilized data from the Canadian Census Health and Environment Cohort of approximately 2.4 million subjects living across Canada. A modest association was observed between mineral dust and cardiovascular mortality. Finally, Wang et al. (2022) used data on 14 million Medicare recipients living in the southeastern United States. The authors reported an association between all-cause mortality and the soil component of $PM_{2.5}$.

5.2 Environmental Justice

Exposure to $PM_{2.5}$ constitutes an environmental justice concern as the adverse effects are borne disproportionately by the most vulnerable, including infants, children and the elderly, people of color, those with low incomes, and those with underlying health conditions (Colmer et al. 2020;

Tessum et al. 2021). These adverse health effects are linked to disproportionately high exposures to pollution sources, often due to residential, school, or work proximity. This increased exposure is compounding because residents in proximity to fossil fuel activity generally are already disproportionately burdened by lower incomes and educational attainment (Davis 2011; Jha & Muller 2018). These and other characteristics of susceptibility and vulnerability qualify such locations as "disadvantaged," or "environmental justice," communities, defined by the California Health and Safety Code Section 39711 as low-income and disproportionately affected by environmental pollution and other hazards. There are three main mechanisms by which these disparities are generated (ALA 2023).

- Increased exposure to pollution due to structural racism and class barriers, especially related to housing, land use, and work conditions
- Fewer advantages and supports related to adequate and protective essential resources, including housing, food, transportation, workplaces
- Higher underlying health conditions and chronic stress related to racism and/or poverty that predispose to greater risks of pollution impacts

5.2.1 Environmental justice and exposure

The United States Environmental Protection Agency (US EPA) has formally concluded that people of color are at greater risk related to exposure to and impacts of particulate matter, and a growing body of literature identifies race as a predominant correlate with these disadvantaged environmental justice communities (Morello-Frosch et al. 2001; Ringquist 2005). U.S. EPA 2019 Section 12.5.4; (Morello-Frosch et al. 2001; Ringquist 2005). Structurally and socially segregated housing related to racist housing policies are major contributors to this disparity (Nardone 2020).

The consequence for Black, Indigenous, Latinx, Asian American, and Middle Eastern communities include elevated exposure to environmental hazards and decreased access to environmental benefits (Marshall 2008). For example, roughly 50% of California's children are Latinx / Hispanic, but constitute 81% of the children in the most burdened census tracts, along with Black children (OEHHA 2018). And, while Latinx / Hispanic and Black residents compose less than 20% and 5%, respectively, of California's elder residents, they compose 46% and 15% of the residents in the highest decile of polluted census tracts, compared to 3% of white elderly residents (OEHHA 2018). This distribution disparity extends to the 20% most polluted census tracts, whose residents are roughly 30% Black and Latinx / Hispanic and 15% Native American, but only 7% white (OEHHA 2018). One study found that these distributions may contribute to up to 40% of the disparity in mean particulate exposure between people of color and white people (Marshall 2008).

This race-based air pollution exposure pattern exists throughout the United States and holds particularly in rail corridors (Miranda et al. 2011; Multnomah County Health Department 2013).

In California, those living in the highest cancer risk zones near major rail yards are more likely to be lower-income or residents of color, or both (A. M. Hricko 2006). Similarly, of those Californians living in rail corridors within what's called the "blast zone" (i.e., within one mile of a railway where a potential oil train derailment could explode), 78% are people of color versus outside of the zone where 57% of residents are people of color (in other words, approximately 22% of residents in the blast zone are white while 43% are white outside the zone). In the City of Richmond, the setting of this present study, the disparity is more pronounced; 89% in the blast zone are people of color compared to 70% outside (CBE 2015).

5.2.2 Environmental justice and health

The U.S. Department of Health and Human Services defines a health disparity as, ''a particular type of health difference closely linked with social, economic, and/or environmental disadvantage. Health disparities adversely affect groups of people who have systematically experienced greater obstacles to health based on their racial or ethnic group" (www.healthypeople.gov). The social and economic impacts of racial and class disparities in exposure are compounded by heightened disparities in adverse health impacts (OEHHA 2018). For example, maternal exposure to air pollution can lead to worse birth outcomes, including low birth weight, preterm birth, and small gestational age for Black and Latinx/Hispanic families than white ones (Gray et al. 2014; Ponce et al. 2005). These adverse birth outcomes can have longer-term implications. In another example, emergency department (ED) visits pursuant to air pollution exposure were found to be disproportionately higher among Black and Latinx populations compared to white ones, including among children (Glad et al. 2012; Grineski et al. 2010), and the risk of asthma attacks is higher in zip codes with high poverty (O'Lenick 2017).

Chronic and acute pollution exposure can lead to serious and acute health effects requiring healthcare services that further disadvantage vulnerable populations. For example, short-term exposure to $PM_{2.5}$ has been found to increase the risk of cardiovascular-related hospitalizations among Medicaid enrollees, even at $PM_{2.5}$ levels below national standards (deSouza 2021). Poor health status itself increases the risk for adverse effects from particulate exposure. Recently, Altman (2023) found that air pollution independently increased asthma exacerbation among urban children in settings with high underlying diseases. These dynamics both indicate and exacerbate social and economic disparities, for example, related to lost work and school days and higher healthcare costs.

Significantly, environmental justice dynamics related to race and socioeconomic standing increase disparities in the risk of premature mortality due to particulate matter (Bell & Ebisu 2012; Medina-Ramón & Schwartz 2008). For example, Kioumourtzoglou et al. (2016) found that among the Medicaid population, people living in predominantly Black communities faced a greater risk of particle pollution-related mortality than those living in predominantly white communities as well as those in neighborhoods with higher levels of poverty and lower educational attainment. Di, et al. (2017) found that, even with higher incomes, Black people faced a higher risk of premature mortality from particulates than their white study counterparts, suggesting that disparities partly arise from the chronic stress of racism. Strong evidence similarly implicates poverty in particulate matter-related mortality (Zeger 2008). Alexeeff (2023) most recently found pronounced increases (21%, 8%) in ischemic heart disease (IHD) and cardiovascular disease (CVD) mortality per 10 $\mu g/m^3$ increase in 1-year mean $PM_{2.5}$, which held for IHD mortality (7%) even at moderate exposure levels that are currently below regulatory standards, joining a body of literature citing currently standards as insufficiently protective.

The impact of proximity to coal and petcoke storage, handling, and transport reinforces the findings of increased vulnerability to adverse health outcomes (Marshall 2008). For example, children attending school near a railyard are likelier to experience adverse respiratory conditions (Spencer-Hwang et al. 2015). Garzón-Galvis et al. (2016) noted, “In 17 out of 18 rail yards in California, a significantly higher proportion of people of color reside within high-risk cancer zones near rail yards than within other areas of the county.” In other words, because fugitive coal and petroleum coke dust emissions are localized, they disproportionately threaten the health, well-being, and communities of people already disadvantaged or made vulnerable by economic, racial, and health disparities.

5.2.3 Local settings

This study points to the likelihood that not only will the discovered coal dust increments be associated with adverse health outcomes but also will constitute environmental justice concerns because the populations most at risk of exposure to the coal dust we detected are also known to have worse baseline health status, lower socio-economic status, and higher exposure to multiple sources of pollution. Further, these residents are more likely to be Black, Indigenous, Latinx/Hispanic, Asian, or Middle Eastern, meaning these disparate impacts deepen racial injustices.

With these considerations in mind, our study results have obvious implications for both Richmond and Oakland. Both Richmond and the neighborhood of West Oakland were selected as the San Francisco Bay Area’s year 1 communities for the state’s Community Air Protection Program. As displayed in Figure 5.1, identification was based on the Air District’s CARE Pollution Index (concentrations of cancer risk, $PM_{2.5}$, and ozone) and the CARE Vulnerability Index (mortality, ED and hospitalization costs, life expectancy).

Figure 5.1 California Air Resources Board CARE Pollution Index and CARE Health Vulnerability Index, with Richmond and West Oakland circled

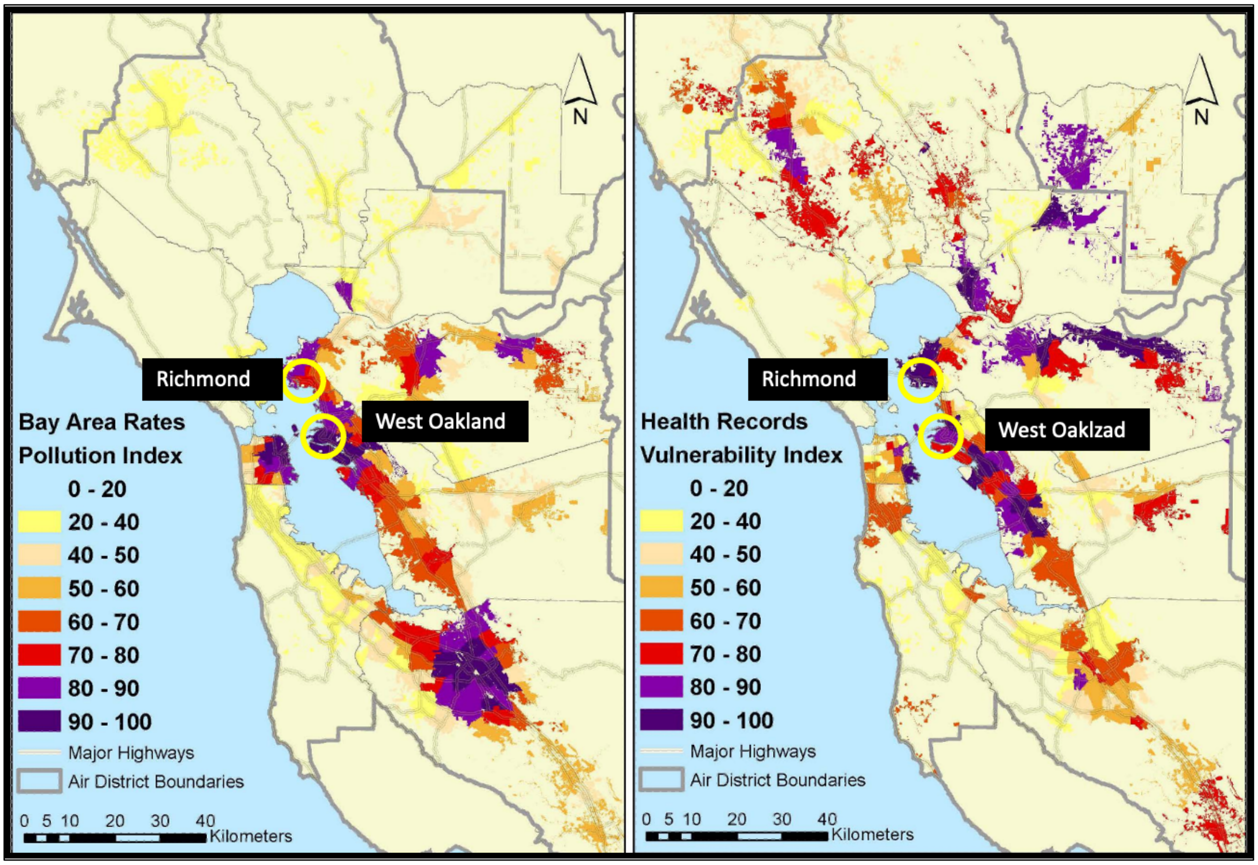

Source: BAAQMD, 2018

Approximately 120,000 people live in the Richmond area. According to the Bay Area Air Quality Management District (BAAQMD), different neighborhoods in Richmond range from 16% to over 33% Black; and from 40% to over 56% percent Latino. Approximately 25,000 people live in West Oakland. Nearly 30% of residents are Black, and over 25 percent are Latino. Both areas have a high degree of low-income residents and significant co-morbidities. As seen with some of the following data, people living in these areas experience "more asthma emergency room visits, higher rates of cardiovascular disease, greater unemployment, lower educational attainment, higher housing cost burden, lower life expectancy and higher incidences of poverty" than in other areas of their respective counties (BAAQMD 2018).

5.3 Environmental Justice and the City of Richmond

The City of Richmond contains what the State of California Health and Safety Code Section 39711 designates as disadvantaged communities, as indicated by the CalEnviroScreen score, a composite measure of environmental exposure, health, and socioeconomic status where higher scores indicate greater pollution burdens. According to CalEnviroScreen (4.0), 9 of Richmond's 22 census tracts (41%) have CalEnviroScreen scores above the 75th percentile. Figure 5.2 places these live, work and learn conditions in the context of coal-related industrial activity.

Figure 5.2 CalEnvrioScreen (4.0) pollution exposure deciles

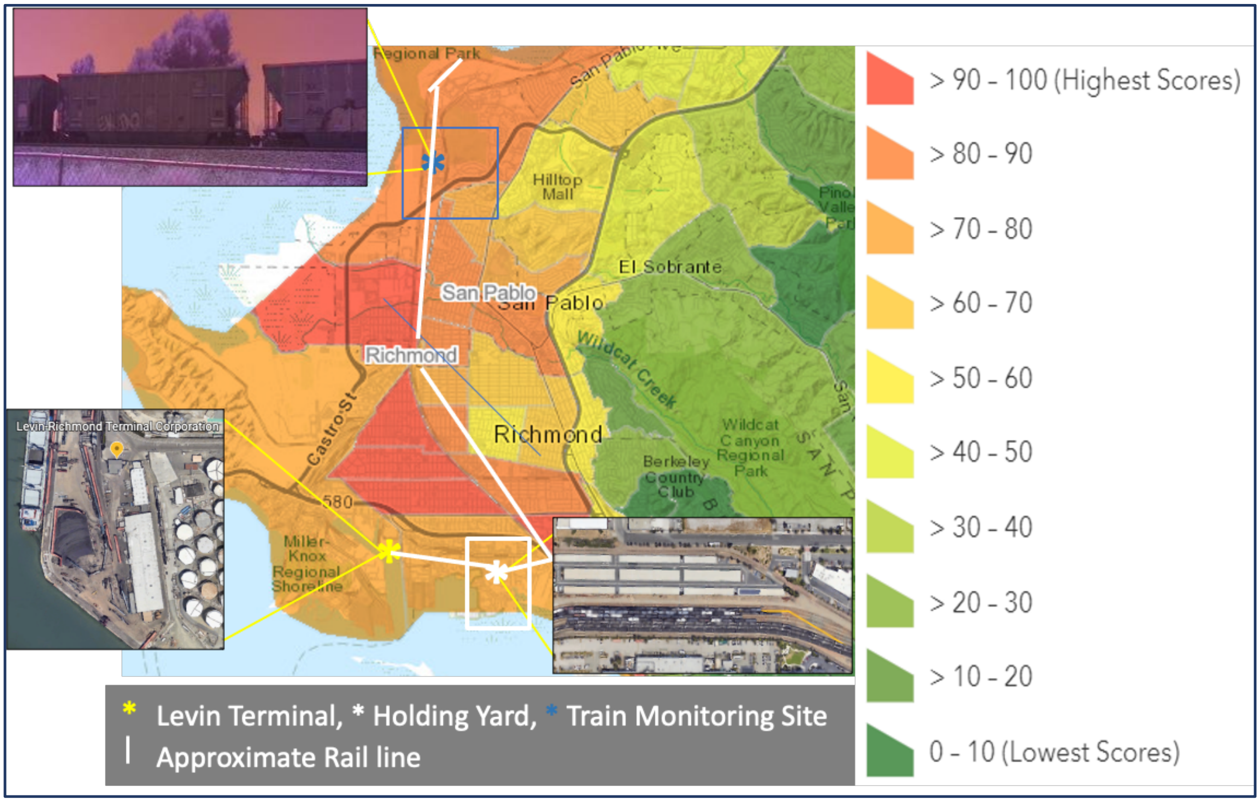

Source: Base map CalEnviroScreen 4.0

5.3.1 Race and pollution exposure, Richmond

There is a statistically significant relationship between the race of residents and whether they live in one of these highly polluted census tracts. Specifically, 56% of Black, Indigenous/Native American Indian, Latinx/Hispanic, Asian/Pacific Islander, and Middle Eastern/North African (BILAM) residents compared to 21% of white residents live in the most polluted census tracts (those in the top 75th percentile according to CalEnviroScreen). Comparing the BILAM and White columns, the table also indicates that 92% of the residents in the most polluted census tracts are BILAM, while 8% are white, meaning for Richmond residents, the odds of living in one of the highest CalEnviroScreen areas (>=75th) is nearly 5 times greater for residents of color than for white residents (Table 5.1).

Table 5.1 Population and race by census tract percentile, CalEnviroScreen Score, Richmond, CA, 2019 estimates

Demographic Row% Col %,)	Total Pop	BILAM*	White	Black	American Indian/ Native Alaskan	Latinx	Asian / PI	Other/ Multi-Race
Richmond	124,433	101,065	23,365	22,958	366	54,051	18,582	5,107
Census Tracts	100%	81%	19%	18%	29%	43%	15%	4%
(22)	100%	100%	100%	100%	100%	100%	100%	100%
CalEnviroScreen	61,510	566,60	4,847	13,832	255	34,100	6,457	2,014
>=75th Score	100%	92%	8%	22%	41%	55%	10%	3%
Census Tract (9)	49%	56%	21%	49%	51%	63%	35%	39%
CalEnviroScreen	62,923	44,405	18,519	9,125	111	19,950	12,124	3,092
<75th Score	100%	71%	29%	15%	0.18%	32%	19%	5%
Census Tract (13)	51%	44%	79%	51%	30%	37%	65%	61%

*BBILAM = Black, Indigenous / Native American Indian, Latinx, Asian/Pacific Islander, Middle Eastern/North African

Source: CalEnviroScreen (4.0)

In terms of the ACAPP study, 7 census tracts in Richmond (30%) are near rail and coal/petcoke storage and handling facilities, and 6 of these (86%) are also among the upper 75th percentile of CalEnviroScreen score sites. Of those living in proximity to rail and coal/petcoke storage and handling, 90% are BILAM residents compared to 10% white (chi-square $p<0.00$); 55% of the residents are Hispanic, and 18% are Black. The age distributions between proximate neighborhoods and more distal ones are also significantly different ($p<0.00$), with the portion of 10-64 year-olds being greater in the study Census Tracts (74% vs. 45%) and among > 65-year-old residents, proportionately more living outside of the proximate zones (32% vs. 68%).

Both environmental exposures and health status are generally worse for residents in these upper 75th percentile areas. For example, as detailed in Table 5.2, risks of asthma Emergency Department (ED) visits, low birth weight, and particulate matter exposure are all worse for those living in a census tract above the 75th percentile CalEnviroScreen.

Table 5.2 Averaged health and air pollution metrics by census tract percentile, CalEnviroScreen, Richmond, CA, 2019 estimates

Average Low High	Asthma ED Visit per 10k pop	Asthma ED Rate Percentile	Low Birth Weight (%)	Low Birth Weight % Percentile	Amt daily max 8 hr [Ozone]	[Ozone] Percentile	Annual mean [PM2.5]
Richmond Census Tracts (22)	112.33	90.05	6.15	67.97	0.03	4.28	9.00
	47.55	52.89	4.74	37.32	.029	3.12	8.78
	158.82	99.33	9.15	97.58	.033	7.52	9.15
Census Tract CalEnviroScreen >=75th Score (9)	135.45	97.19	6.77	84.05	0.03	3.94	9.03
	102.33	93.21	4.97	51.49	.029	3.12	8.15
	157.78	99.26	9.15	97.58	.033	7.52	9.15
Census Tract CalEnviroScreen <75th Score (13)	96.92	85.28	5.53	57.25	0.03	4.51	8.98
	47.55	52.89	4.39	37.32	.029	3.12	8.78
	158.82	99.33	9.00	77.05	.032	6.38	9.11

*For each census tract percentile category, there was one extreme outlier possibly due to recording or measurement error; these outliers were not included in the averaging or ranges

Source: CalEnviroScreen (4.0)

5.3.2 Birth outcomes: Low birth weight and preterm birth

The average low birth rate for residents in census tracks near rail, storage, and handling infrastructure for coal and/or petcoke is 8.1 (range: 6.2 - 10.4), or 18% higher than the rate in Richmond as a whole, and 30% higher than Contra Costa County. Similarly, and as detailed in Appendix 4, for preterm births (PTB), the average rate for residents in census tracks near rail, storage, and handling facilities for coal and/or petcoke is 9.4 (range: 7.8 - 11.2) or 7% higher than the rate in Richmond as a whole, and 18% higher than Contra Costa County. Rates seemed to be influenced by economic status in a manner fairly consistent between Richmond and Contra Costa County (Appendix 4). For example, the lowest LBW and PTB rates are among those privately insured (Richmond/Contra Costa: 5.8% / 5.1% LBW and 7.0% / 7.1% PTB). The highest rates for LBW and PTB were recorded among government program recipients other than Medi-Cal (Richmond/Contra Costa: 13.2% / 16.0%; 15.1% / 19.2%).

5.3.3 Mortality

Generally, the population in the study area carries the highest rate of mortality burden in comparison to Richmond and Contra Costa County. As detailed in Table 3, across all race groups where data is available, 76% of the time it is the populations in the study zone in proximity to rail, storage, and handling facilities for coal experienced the highest rate. For all-cause mortality, the average rate for these proximate census tracts was 17% and 26% greater than for Richmond as a whole and Contra Costa County, respectively. This disparity was pronounced for the Black community, where the study site rate for all-cause and all-cancer mortality was roughly 35% greater, nearly 40% greater for stroke, and roughly 66% greater for respiratory disease mortality.

5.3.4 Emergency departments and hospitalizations

Compared with Contra Costa County, Richmond zip codes and the monitoring areas., in particular 94801, consistently post higher ED discharge rates. Asthma disparities are especially pronounced, with the total rate being approximately 65% more and approximately 40 - 55% greater when considering race and 60% - 70% greater when considering age. ED discharges for respiratory conditions were overall 60% higher in 94801 than for the county (see details in Appendix 4).

5.4 Environmental Justice and the City of Oakland

The present study's policy context includes considering a proposed coal export terminal in Oakland. A previously issued report, An Assessment of the Health and Safety Implications of Coal Transport Through Oakland (Public Health Advisory Panel on Coal (PHAP) 2016), identified similar health and environmental justice concerns present in Richmond, for example, noting that West Oakland’s Pollution Vulnerability Index (PVI, a score based upon level of health risk from air pollution) was among the highest quintile of PVI (80 – 100 percentile), associated with three years of life lost for people living in these areas (Garzón-Galvis et al. 2016).

West Oakland faces similar questions regarding coal and rail activity and particulate matter impacts. Modeling conducted by Gray (2017) concluded that emissions from the proposed terminal would substantially contribute to elevated levels of fine particulate matter over a large area surrounding the facility, with long-term average $PM_{2.5}$ concentrations increasing by at least 0.5 $\mu g/m^3$ over an area of 3.5 - 5.4 square kilometers surrounding the facility depending upon the route. A 2016 rough estimate drew a similar conclusion (PHAP 2016).

The report identified that any such impacts would exacerbate already significant air pollution-related hazards, further noting that West Oakland residents living within approximately 1500 feet of the terminal already experience levels of $PM_{2.5}$ that are close to the existing state and federal standards and above the WHO health-based standard. The Alameda County Public Health Department confirms that the Oakland population living within one mile of rail lines is markedly different demographically than that living farther away, with a higher percentage of people of color, children, and adolescents, and people living in poverty (ACPHD 2016). Further, many important community resources and sensitive sites (schools, parks, community services) are located near the rails (Figure 5.3).

Figure 5.3 Oakland rail corridors, exposure bands, and sensitive receptor sites

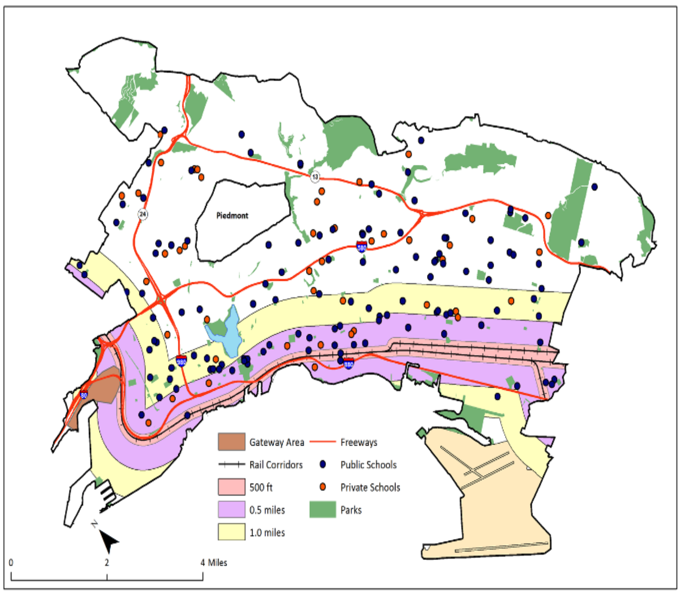

Source: CAPE, with rail data from CalTrans, parks data from CPAD 2015b, Gateway area from Oakland Redevelopment Agency, schools from CDE.

These conditions leave this community more impacted by pollution, health disparities, and environmental justice concerns. For example, Oakland census tracts within 500 feet of rail lines, compared to elsewhere in Oakland and Alameda County, have significantly higher mortality rates from all causes, as well as specifically from cancer, heart disease, stroke, and chronic lower respiratory disease (ACPHD 2016) (ACPHD 2015).

5.4 Discussion

This review links chronic and acute exposure to fine and coarse particulate matter with adverse health outcomes. It also indicates that the environmental justice communities in Richmond and Oakland are likely to experience heightened adverse health effects due to proximity to coal export infrastructure and activity and due to higher underlying health conditions and social determinants. As the Alameda County Public Health Department found, “Any additional sources of air pollution will have a significantly greater impact in an area already disproportionately burdened by multiple sources of air pollution and with high rates of emergency room visits and hospitalization for asthma and cancer risk from existing pollution” (ACPHD 2015). The American Lung Association State of the Air Assessment reinforces the idea that these locales are already at a pollution tipping point. It ranks the San Jose - San Francisco - Oakland area as having the fourth worst $PM_{2.5}$ pollution in the country for both year-round and short-term particle pollution, and

Contra Costa and Alameda County both received a grade of "F" for their air quality (ALA b 2022). Further, public health and environmental justice implications are likely to be exacerbated by climate change, where higher temperatures interact with augmented pollution generation and adverse health effects to potentially increase the impacts of $PM_{2.5}$ related to coal transport, storage, and handling (Kioumourtzoglou 2016; Jacobson 2008; Keswani 2022).

Adverse health outcomes associated with $PM_{2.5}$ are also expensive. A BAAQMD health impact assessment of the San Francisco Bay Area estimated that the per capita cost of air pollution health burdens ran on the order of $2000 and $1,750 for Contra Costa and Alameda County residents, respectively (Tanrikulu 2011). Conversely, reducing air pollution can have great economic and societal benefits. BAAQMD found that for every reduction of 1 $\mu g/m^3$, half a billion dollars could be accrued through the benefits of averted mortality and that the total benefit of reducing current $PM_{2.5}$ concentrations to a "clean background" level was $13.5 billion (Tanrikulu 2011).

6. Conclusions

The present study examined the extent to which $PM_{2.5}$ is generated by rail transport of coal and its storage and handling in the City of Richmond, California, specifically at the Levin Terminal, nearby rail holding yard, and affiliated rail corridor. It also considers whether these emissions increase community exposure and bear health implications for the local community. Specifically, in periods between October 2019 and October 2022, the present study measured coal-related $PM_{2.5}$ pertaining to: 1) rail conveyance of coal through Richmond; 2) coal train car storage at the holding yard; 3) coal and petcoke storage and handling activities at the Levin Terminal; and 4) exposure in nearby communities.

There are several important findings from the present study's extensive monitoring data. Even so, by not including coarse particles (PM_{10}- $PM_{2.5}$) and ultrafine particles (PM < 0.1 microns), both of which have important health effects, this study underestimates the total impact.

In particular, the study found that rail conveyance of coal significantly increases ambient concentrations of $PM_{2.5}$. The average (5-minute) change from passing coal trains adds approximately 8.3 $\mu g/m^3$ (95% CI = 6.4, 10.3) to the ambient $PM_{2.5}$, with midpoint estimates ranging from 5 to 12 $\mu g/m^3$. Full coal cars contribute approximately 2 to 3 $\mu g/m^3$ of $PM_{2.5}$ more than freight trains. Rail transit of unloaded cars also increases ambient $PM_{2.5}$ concentrations. Unloaded coal cars tended to add 2 $\mu g/m^3$ of $PM_{2.5}$. Storage of coal and coal cars at the rail yard significantly increases ambient concentrations of $PM_{2.5.}$ Full coal train cars kept at the train yard contribute 2 to 3 $\mu g/m^3$ (one-hour average) of $PM_{2.5}$ above background concentrations, often 0.2 $\mu g/m^3$ greater than those of freight trains. Empty coal cars stored at the yards contributed to ambient $PM_{2.5}$ by an increment of 0.2 $\mu g/m^3$ over freight trains during days of relatively calm winds. Terminal operations involving coal transport, storage, and handling significantly increase community exposure to ambient $PM_{2.5}$ at concentrations ranging from 0.1 to 0.6 $\mu g/m^3$. This presence of coal in the community was independently detected and corroborated by 1) passive samplers, 2) adhesive carbon tape, and 3) DRUM (Davis Rotating Unit for Monitoring).

These quantified $PM_{2.5}$ increments have significant health and environmental justice implications for the exposed population. Hundreds of studies have reported causal associations between $PM_{2.5}$ and serious health effects, including premature mortality and hospitalization. Effects have been documented from hourly, daily, and annual exposures. In addition, dozens of studies document significant adverse health effects after exposure to $PM_{2.5}$ and coarse particles from fugitive dust. Exposure to $PM_{2.5}$ constitutes an environmental justice concern as the adverse effects are borne disproportionately by the most vulnerable, including infants, children and the elderly, people of color, those with low incomes, and those with underlying health conditions.

These adverse health effects are linked to disproportionately high exposures to pollution sources, often due to residential, school, or work proximity.

Understanding the contribution of coal transport, storage, and handling in urban populations has broad implications. Inevitable dispersion of $PM_{2.5}$ will increase population exposure over a much wider area. Further, since the shipment of coal by train occurs throughout the world and often involves urban areas, it represents a significant global and local public health hazard that extends to matters of environmental and racial justice. Recent derailments also make clear the importance of contributing to the general body of knowledge concerning rail activity. Given that the industrial activity assessed in this study is for the ultimate purpose of burning fossil fuels, it is relevant to note that these same communities are also at greater risk from the impacts of climate change.

Most recently, Josey et al. (2023) found that reducing $PM_{2.5}$ concentrations would not only benefit the full community through decreases in mortality risks but would also provide larger relative benefits to those with the highest mortality risks. Since the latter includes people of color and those disadvantaged economically, $PM_{2.5}$ reduction can thereby decrease health disparities while protecting health for all.

In conclusion, studies on specific sources of pollution, such as the present one, open pathways to emission reductions that might not otherwise have been pursued. We therefore recommend increasing investment in this type of study that integrates AI-detection and visualization monitoring with multiple speciation analyses and study designs for targeted assessments to secure health, health equity, and environmental justice.

7. References

Ångström, Anders. (1929) On the atmospheric transmission of sun radiation and on dust in the air. Geografiska Annaler 11: 156–66. https://doi.org/10.2307/519399.

ACPHD (2016) Alameda County Public Health Department, Community Assessment, Planning, and Evaluation.

Adar SD, Filigrana PA, Clements N, Peel JL (2014) Ambient coarse particulate matter and human health: A systematic review and meta-analysis. Current Environmental Health Reports 1(3): 258–274. https://doi.org/10.1007/s40572-014-0022-z

Aghababaeian H, Ostadtaghizadeh A, Ardalan A, et al. (2021) Global health impacts of dust storms: a systematic review. Environmental Health Insights 2021;15. doi:10.1177/11786302211018390

Akaoka K, McKendry I, Saxton J, Cottle PW (2017) Impact of coal-carrying trains on particulate matter concentrations in South Delta, British Columbia, Canada. Environmental Pollution 223:376–383. https://doi.org/10.1016/j.envpol.2017.01.034

Alameda County Public Health Department (2008) Life and Death from Unnatural Causes: Health and Social Inequity in Alameda County.

Alexeeff SE, Deosaransingh K, Van Den Eeden S, Schwartz J, Liao NS, Sidney S (2023) Association of long-term exposure to particulate air pollution with cardiovascular events in California. JAMA Network 6(2):e230561. doi:10.1001/jamanetworkopen.2023.0561

Altman, MC et al. (2023) Associations between outdoor air pollutants and non-viral asthma exacerbations and airway inflammatory responses in children and adolescents living in urban areas in the USA: A retrospective secondary analysis. The Lancet Planetary Health January, 7(1); E33-E44. DOI: https://doi.org/10.1016/S2542-5196(22)00302-3

American Lung Association. Disparities in the Impact of Air Pollution. Accessed March 9, 2023 at https://www.lung.org/clean-air/outdoors/who-is-at-risk/disparities

Aneja VP, Isherwood A, Morgan P (2012) Characterization of particulate matter (PM_{10}) related to surface coal mining operations in Appalachia. Atmospheric Environment 54:496–501.

AQ-SPEC: http://www.aqmd.gov/aq-spec, last access: 6 December 2022.

BAAQMD (2018) San Francisco Bay Area Community Health Protection Program: Improving Neighborhood Air Quality Final Submittal: Public Process for Determination of Recommended Communities. Bay Area Air Quality Management District, August 1.
https://www.baaqmd.gov/~/media/files/ab617-community-health/2018_0704_draft-submittal_master-pdf.pdf?la=en

Barkjohn KK, Gantt, B, Clements AL (2021) Development and Application of a United States-wide correction for $PM_{2.5}$ data collected with the PurpleAir sensor. Atmospheric Measurement Techniques 4(6). https://doi.org/10.5194/amt-14-4617-2021

Barkjohn KK, Holder AL, Frederick SG, Clements AL (2022) Correction and Accuracy of PurpleAir $PM_{2.5}$ Measurements for Extreme Wildfire Smoke. Sensors 22, no. 24 (January): 9669. https://doi.org/10.3390/s22249669.

Baruya P (2012) Losses in the coal supply chain. IEA Clean Coal Centre. https://usea.org/sites/default/files/122012_Losses%20in%20the%20coal%20supply%20chain_ccc212.pdf

Bell M L, Ebisu K (2012) Environmental inequality in exposures to airborne particulate matter components in the United States. Environmental health perspectives 120(12), 1699–1704. https://doi.org/10.1289/ehp.1205201

Bell ML, Zanobetti A, & Dominici F (2013) Evidence on vulnerability and susceptibility to health risks associated with short-term exposure to particulate matter: a systematic review and meta-analysis. American Journal of Epidemiology 178(6), 865. https://doi.org/10.1093/aje/kwt090

Bhaskaran K, Hajat S, Armstrong B, Haines A, Herrett E, Wilkinson P, & Smeeth L (2011) The effects of hourly differences in air pollution on the risk of myocardial infarction: Case crossover analysis of the MINAP database. BMJ 343, d5531. https://doi.org/10.1136/bmj.d5531

BNSF Railway (2011) Coal dust frequently asked questions [2011 version] No longer available.

Bond TC, Bergstrom RW (2006) Light Absorption by Carbonaceous Particles: An Investigative Review. Aerosol Science and Technology 40 (January): 27–67. https://doi.org/10.1080/02786820500421521

Brunekreef B, Strak M, Chen J, et al. (2021) Mortality and Morbidity Effects of Long-Term Exposure to Low-Level $PM_{2.5}$, BC, NO2, and O3: An Analysis of European Cohorts in the ELAPSE Project. Research Reports: Health Effects Institute 208.

Cahill TA, Cahill TM, Barnes DE, et al. (2011) Inorganic and organic aerosols downwind of California's Roseville Railyard. Aerosol Science and Technology 45:9, 1049-1059. DOI:10.1080/02786826.2011.580796

California Air Resources Board (2008) Health Risk Assessment for the BNSF San Bernardino Railyard. Appendix F.

California Health and Safety Code Section 39711. https://legiscan.com/CA/text/SB535/id/665273

CBE (2015) Crude Injustice on the Rails (p. 30). Communities for a Better Environment and Forest Ethics. https://www.cbecal.org/wp-content/uploads/2015/07/Crude-Injustice-on-the-Rails.pdf

Chen D, Zhang F, Yu C, Jiao A, Xiang Q, Yu Y, Mayvaneh F, Hu K, Ding Z, Zhang Y (2019) Hourly associations between exposure to ambient particulate matter and emergency department visits in an urban population of Shenzhen, China. Atmospheric Environment 209:78–85. https://doi.org/10.1016/j.atmosenv.2019.04.021

Chen R, Yin P, Meng X et al. (2019) Associations between coarse particulate matter air pollution and cause-specific mortality: a nationwide analysis in 272 Chinese Cities. Environment Health Perspectives 127:017008. doi: 10.1289/EHP2711.

Chen TT, Zhan ZY, Yu YM, et al. (2020) Effects of hourly levels of ambient air pollution on ambulance emergency call-outs in Shenzhen, China. Environmental Science and Pollution Research International 27(20): 24880–24888. https://doi.org/10.1007/s11356-020-08416-w

Chen Weng Y, Chiu Y, Yang C (2015) Short-term effects of coarse particulate matter on hospital admissions for cardiovascular diseases: a case-crossover study in a tropical city. Journal of Toxicology and Environmental Health 78(19):1241-53. doi: 10.1080/15287394.2015.1083520. Epub 2015 Sep 25.

Crouse DL, Sajeev Philip, Van Donkelaar Aaron, Martin RV, et al. (2016) A new method to jointly estimate the mortality risk of long-term exposure to fine particulate matter and its components. Scientific Reports 6: 18916.

Crouse DL, Erickson AC, Christidis T, Pinault L, Van Donkelaar A, Li C, Meng J, Martin RV, Tjepkema M, Hystad P, Burnett R, Pappin A, Brauer M, Weichenthal S (2020) Evaluating the sensitivity of $PM_{2.5}$-mortality associations to the spatial and temporal scale of exposure assessment. Epidemiology Mar;31(2):168-176. doi: 10.1097/EDE.0000000000001136. PMID: 31693516

Davis LW (2011) The Effect of power plants on local housing values and rents. The Review of Economics and Statistics 93(4), 1391–1402. https://doi.org/10.1162/REST_a_00119

Davis E, Malig B, Broadwin R, et al. (2020) Association between coarse particulate matter and inflammatory and hemostatic markers in a cohort of midlife women. Environ Health Nov 5;19(1):111. doi: 10.1186/s12940-020-00663-1.

deSouza P, Braun D, Parks RM, Schwartz J, Dominici F, Kioumourtzoglou MA (2021) Nationwide study of short-term exposure to fine particulate matter and cardiovascular hospitalizations among medicaid enrollees. Epidemiology Jan;32(1):6-13. doi: 10.1097/EDE.0000000000001265. PMID: 33009251; PMCID: PMC7896354.

Di Q, Wang Y, Zanobetti A, et al. (2017) Air pollution and mortality in the Medicare population. N. Engl. J. Med 376, 2513–2522.

Diaz J, et al. (2017) Saharan dust intrusions in Spain: Health impacts and associated synoptic conditions. Environmental Research 156: 455-467 DOI: 10.3390/ijerph110201914

DSITIA (2015) Initial Report on the Independent Review of Rail Coal Dust Emissions Management Practices in the NSW Coal Chain.

Dubovik O, Holben B, Eck TF, Smirnov A, Kaufman YJ, King MD, Tanre D, Slutsker I (2002) Variability of absorption and optical properties of key aerosol types observed in worldwide locations. Journal of the Atmospheric Sciences 59: 590–608. https://doi.org/10.1175/1520-0469(2002)059<0590:voaaop>2.0.co;2.

Fu J, Liu Y, Zhao Y, et al. (2023) Hourly valley concentration of air pollutants associated with increased acute myocardial infarction hospital admissions in Beijing, China. Atmosphere 14, 27. doi.org/10.3390/atmos14010027

Fuller R, Landrigan PJ, Balakrishnan K, Bathan G, Bose-O'Reilly S, Brauer M, Caravanos J, Chiles T, Cohen A, Corra L, Cropper M, Ferraro G, Hanna J, Hanrahan D, Hu H Hunter D, Janata G, Kupka R, Lanphear B, Yan C (2022) Pollution and health: A progress update. The Lancet Planetary Health 6(6):e535-e547. https://doi.org/10.1016/S2542-5196(22)00090-0

Galvis B, Bergin M, Boylan J, et al. (2015) Air quality impacts and health-benefit valuation of a low-emission technology for rail yard trains in Atlanta Georgia. Science of the Total Environment 533:156–164.

Garzón-Galvis C, Harris L, Levitt Z, Ratner J (2016) Making a good move for health: A health impact assessment of select strategies of the Alameda County goods movement plan.

Glad JA, Brink LL, Talbott EO, Lee PC, Xu X, Saul M, & Rager J (2012). The Relationship of ambient ozone and $PM_{2.5}$ levels and asthma emergency department visits: possible influence of gender and ethnicity. Archives of Environmental & Occupational Health 67(2), 103–108. https://doi.org/10.1080/19338244.2011.598888

Gray AH (2017) Modeling PM Air Quality Impacts of the Proposed OBOT Facility. Gray Sky Solutions San Rafael, California October 6.

Gray SC, Edwards SE, Schultz BD, & Miranda ML (2014) Assessing the impact of race, social factors and air pollution on birth outcomes: a population-based study. Environmental Health 13(1), 4. https://doi.org/10.1186/1476-069X-13-4

Grineski SE, Staniswalis JG, Peng Y, & Atkinson-Palombo C (2010) Children's asthma hospitalizations and relative risk due to nitrogen dioxide (NO2): effect modification by race, ethnicity and insurance status. Environmental Research 110(2), 178. https://doi.org/10.1016/j.envres.2009.10.012

Hatch JR, Affolter RH, & Davis FD (1979) Chemical analyses of coal from the Blackhawk formation, Wasatch plateau Coal Field. Carbon, Emery, and Sevier counties, Utah, Utah Geological and Mineral Survey, Utah Department of Natural Resources. Special Studies 49 August.

Hatch C (2008) Final Report Environmental Evaluation of Fugitive Coal Dust Emissions from Coal Trains Goonyella, Blackwater and Moura Coal Rail Systems Queensland Rail Limited Report no. H327578-N00-EE00.00. (March 31). https://majorprojects.planningportal.nsw.gov.au/prweb/PRRestService/mp/01/getContent?AttachRef=MP09_0024%2120190814T054754.584%20GMT

Higginbotham N, Ewald B, Mozeley F, Whelan J (2013) Coal Train Signature Study, Briefing Paper Prepared for Coal Terminal Action Group Dust and Health Committee. Coal Terminal Action Group (August):pp1-26. https://cdn.newsnow.io/storypad-bzDwk8TrKQYKjEefACKcS8/CoalTrainSignatureReportAug2013.pdf

Higginbotham N (2014) Expert Report—Nick Higginbotham Public Health Impacts of T4 (pp. 1–65). https://www.ipcn.nsw.gov.au/resources/pac/media/files/pac/projects/2012/09/port-waratah-coal-terminal-4/edo-nsw-on-behalf-of-hcec/27a-expert-report-nick-higginbothampdf.pdf

Hricko AM (2006) Guest editorial: ships, trucks, and trains: Effects of goods movement on environmental health. Environmental Health Perspectives 114(4), A204–A205. https://doi.org/10.1289/ehp.114-a204

Hricko A, Rowland G, Eckel S, Logan A, Taher M, Wilson J (2014) Global trade, local impacts: lessons from California on health impacts and environmental justice concerns for residents living near freight rail yards. International Journal of Environmental Research and Public Health 11(2):1914-1941. https://doi.org/10.3390/ijerph110201914

HealthyPeople.gov. Disparities [cited 2023 March 18] Available from: http://www.healthypeople.gov/2020/about/disparitiesAbout.aspx.

Ihalainen M, Lind T, Torvela T, Lehtinen KEJ, Jokiniemi J (2012) A Method to Study Agglomerate Breakup and Bounce During Impaction. Aerosol Science and Technology 46: 990–1001. doi.org/10.1080/02786826.2012.685663

IPCC (2022) Climate Change 2022: Impacts, Adaptation and Vulnerability. International Panel on Climate Change. https://www.ipcc.ch/report/ar6/wg2/

Jacobson MZ (2008) On the causal link between carbon dioxide and air pollution mortality. Geophysical Research Letters 35(3). https://doi.org/10.1029/2007GL031101.

Jaffe DA, Hof G, Malashanka S, Putz J, Thayer J, Fry JL, Ayres B, & Pierce JR (2014) Diesel particulate matter emission factors and air quality implications from in–service rail in Washington State, USA. Atmospheric Pollution Research 5(2), 344–351. https://doi.org/10.5094/APR.2014.040

Jaffe D, Putz J, Hof G, Hof G, Hee J, Lommers-Johnson DA, Gabela F, Fry JL, Ayres B, Kelp M, Minsk M (2015) Diesel particulate matter and coal dust from trains in the Columbia River Gorge, Washington State, USA. Atmospheric Pollution Research 6(6):946–952. https://doi.org/10.1016/j.apr.2015.04.004

Jha A, Muller M (2017) Handle with Care: The Local Air Pollution Costs of Coal Storage. National Bureau of Economic Research Report No. w23417. doi: 10.3386/w23417

Jha A, Muller NZ (2018) The local air pollution cost of coal storage and handling: Evidence from U.S. power plants. Journal of Environmental Economics and Management, Elsevier, vol. 92(C), 360-396.

Josey KP, Delaney SW, Wu X, Nethery RC, DeSouza P, Braun D, Dominici F (2023) Air Pollution and Mortality at the Intersection of Race and Social Class. NEJM 388:1396-1404 DOI: 10.1056/NEJMsa2300523

Katestone Environmental Pty Ltd (2013) Pollution Reduction Program 4.2 Particulate Emissions from Coal Trains. Australian Rail Track Corporation Pty Ltd 1-82.

Keswani A, Akselrod H, Anenberg SC (2022) Health and clinical impacts of air pollution and linkages with climate change. NEJM Evidence 1(7). https://evidence.nejm.org/doi/full/10.1056/EVIDra2200068

Kim J, Kim H, Kweon J (2015) Hourly differences in air pollution on the risk of asthma exacerbation. Environmental Pollution 203:15–21. https://doi.org/10.1016/j.envpol.2015.03.040

Kioumourtzoglou MA, Schwartz J, James P, Dominici F, Zanobetti A (2016) $PM_{2.5}$ and mortality in 207 US cities: modification by temperature and city characteristics. Epidemiology 27: 221-227.

Krall JR, G. Anderson B, Dominici F, Bell, ML, Peng RD (2013) Short-term exposure to particulate matter constituents and mortality in a national study of US Urban communities. Environmental health perspectives 121:1148–1153.

Lee, Joong Won, Hee Jae Lee, Young-Joo Lee, Yong-beom Lim, Woo Jong Sim, Ji-Hye Jang, Hye-Ryeon Heo, Hyun Joung Lim, Ji-Won Jung, and Jin Sik Kim (2021) Determination of Genotoxicity Attributed to Diesel Exhaust Particles in Normal Human Embryonic Lung Cell (WI-38) Line. Biomolecules 11, no. 2: 291. doi.org/10.3390/biom11020291

Lelieveld J, JS Evans, M Fnais, D Giannadaki, and A. Pozzer (2015) The contribution of outdoor air pollution sources to premature mortality on a global scale. Nature 525: 367–71.

Liu C, Cai J, Chen R, et al. (2022) Coarse particulate air pollution and daily mortality: a global study in 205 cities. American Journal of Respiratory and Critical Care Medicine 206(8):999-1007. doi: 10.1164/rccm.202111-2657OC.

Liu L, Song F, Fang J, Wei J, Ho HC, Song, Y Zhang, Y Wang L, Yang Z, Hu C, & Zhang Y (2021) Intraday effects of ambient PM1 on emergency department visits in Guangzhou, China: a case-crossover study. Science of The Total Environment 750: 142347. https://doi.org/10.1016/j.scitotenv.2020.142347

Marshall JD (2008) Environmental inequality: air pollution exposures in California's South Coast Air Basin. Atmospheric Environment 42(21), 5499–5503. https://doi.org/10.1016/j.atmosenv.2008.02.005

McDuffie E, Martin R, Brauer M (2021) A Global Assessment of Burden of Disease from Exposure to Major Air Pollution Sources: Synopsis of Research Report 210 December (p. 4). https://www.healtheffects.org/system/files/mcduffie-rr-210-statement.pdf

Medina-Ramón M & Schwartz J (2008) Who is more vulnerable to die from ozone air pollution? Epidemiology 19(5), 672–679. https://doi.org/10.1097/EDE.0b013e3181773476

Meyer R (2019) A Major but Little-Known Supporter of Climate Denial: Freight Railroads. The Atlantic. December;13. 12-13T17:43:47Z; https://www.theatlantic.com/science/archive/2019/12/freight-railroads-funded-climate-denial-decades/603559/

Mikati I, Benson AF, Luben TJ, Sacks JD, Richmond-Bryant J (2018) Disparities in distribution of particulate matter emission sources by race and poverty status. American Journal of Public Health 108(4):480–485. https://doi.org/10.2105/AJPH.2017.304297

Miranda ML, Edwards SE, Keating MH, & Paul CJ (2011) Making the environmental justice grade: the relative burden of air pollution exposure in the United States. International Journal of Environmental Research and Public Health 8(6), 1755–1771. https://doi.org/10.3390/ijerph8061755

Morello-Frosch R, Pastor M, & Sadd J (2001) Environmental justice and Southern California's "riskscape" the distribution of air toxics exposures and health risks among diverse communities. Urban Affairs Review 36(4), 551–578. https://doi.org/10.1177/10780870122184993

Multnomah County Health Department L (2013) The Human Health Effects of Rail Transport of Coal Through Multnomah County, Oregon: A Health Analysis and Recommendations for Further Action (p. 23). https://multco-web7-psh-files-usw2.s3-us-west-2.amazonaws.com/s3fs-public/health/documents/coal_report_final_021413.pdf

Nardone A, Casey JA, Morello-Frosch R, Mujahid M, Balmes JR, Thakur N (2020) Associations between historical residential redlining and current age-adjusted rates of emergency department visits due to asthma across eight cities in California: an ecological study. Lancet Planetary Health 4(1):e24-e31.

Nirel R, Adar SD, Dayan U Vakulenko-Lagun B, Golovner M, Levy I, Alon Z, Peretz A (2018) Fine and Coarse Particulate Matter Exposures and Associations with Acute Cardiac Events among Participants in a Telemedicine Service: A Case-Crossover Study. Environmental Health Perspectives 126(9):97003. doi.org/10.1289/EHP2596

O'Kane M (2015) Initial Report on the Independent Review of Rail Coal Dust Emissions Management Practices in the NSW Coal Chain. NSW Chief Scientist & Engineer November 30. https://www.chiefscientist.nsw.gov.au/__data/assets/pdf_file/0009/79884/Initial-Report_Review-rail-coal-dust-emissions.pdf

O'Lenick CR, et al. (2017) Assessment of neighborhood-level socioeconomic status as a modifier of air pollution-asthma associations among children in Atlanta. J Epi Comm Health 71(2):129-136.

OEHHA (2015) Risk Assessment Guidelines: Guidance Manual for Preparation of Health Risk Assessments, Appendices A-N. Air Toxics Hot Spots Program, Office of Environmental Health Hazards Assessment. February https://oehha.ca.gov/media/downloads/crnr/2015guidancemanual.pdf

OEHHA (2018) Analysis of Race/Ethnicity, Age, and CalEnviroScreen 3.0 Scores p19. Office of Environmental Health Hazard Assessment, California Environmental Protection Agency. https://oehha.ca.gov/media/downloads/calenviroscreen/document-calenviroscreen/raceageces3analysis.pdf

Ostro B, Feng WY, Broadwin R, Green S, Lipsett M (2007) The effects of components of fine particulate air pollution on mortality in California: results from CALFINE. Environmental health perspectives 115:13–19.

Ostro B, et al. (2011) Long-term exposure to constituents of fine particulate air pollution and mortality: results from the California Teachers Study. Environmental health perspectives 119:A242.

Ostro B, Hu J, Goldberg D, Reynolds P, Hertz A, Bernstein L, Kleeman MJ (2015) Associations of mortality with long-term exposures to fine and ultrafine particles, species and sources: results from the California Teachers Study Cohort. Environmental Health Perspectives 123(6):549–556. https://doi.org/10.1289/ehp.1408565

Ostro B, Malig B, Hasheminassab S, et al (2016) Associations of source-specific fine particulate matter with emergency department visits in California. American jJurnal of Epidemiology 184:450–459.

Ostro B, Awe Y, Sanchez-Triana E (2021) "When the Dust Settles." World Bank Publications - Reports 36267, The World Bank Group, Washington DC. https://openknowledge.worldbank.org/handle/10986/36267

Ouimette JR, Malm WC, Schichtel BA, Sheridan PJ, Andrews E, Ogren JA, Arnott WP (2022) Evaluating the PurpleAir monitor as an aerosol light scattering instrument. Atmospheric Measurement Techniques 15:655–676. https://doi.org/10.5194/amt-15-655-2022

Pappin AJ, Christidis T, Pinault LL, Crouse DL, Brook JR, Erickson A, Hystad P, Li C, Martin RV, Meng J, Weichenthal S, Van Donkelaar A, Tjepkema M, Brauer M, Burnett RT (2019) Examining the shape of the association between low levels of fine particulate matter and mortality across three cycles of the Canadian Census Health and Environment Cohort. Environmental health perspectives 127, Article 107008. 10.1289/EHP5204

Parker JD, Kravets N, Vaidyanathan A (2018) Particulate matter air pollution exposure and heart disease mortality risks by race and ethnicity in the United States: 1997 to 2009 National Health Interview Survey with mortality follow-up through 2011. Circulation Apr 17;137(16):1688-1697. doi: 10.1161/CIRCULATIONAHA.117.029376. Epub 2017 Dec 13. Erratum in: Circulation Aug 7;138(6):e124. PMID: 29237717; PMCID: PMC5908251.

Peters A, Dockery DW, Muller JE, & Mittleman MA (2001) Increased particulate air pollution and the triggering of myocardial infarction. Circulation 103(23), 2810–2815. https://doi.org/10.1161/01.cir.103.23.2810

Ponce NA, Hoggatt KJ, Wilhelm M, & Ritz B (2005) Preterm birth: the interaction of traffic-related air pollution with economic hardship in Los Angeles neighborhoods. American Journal of Epidemiology 162(2), 140–148. https://doi.org/10.1093/aje/kwi173

Prakash BB, Kecojevic V, Lashgari A (2018) Analysis of dust emission at coal train loading facility. International Journal of Mining. Reclamation and Environment 32(1):56-74. http://dx.doi.org/10.1080/17480930.2016.1253138

PHAP (2016) An Assessment of the Health and Safety Implications of Coal Transport through Oakland. Public Health Advisory Panel on Coal; Oakland, California June 14.

Ringquist EJ (2005) Assessing evidence of environmental inequities: A meta-analysis. Journal of Policy Analysis and Management 24(2), 223–247. https://doi.org/10.1002/pam.20088

Rogers Z, Whelan J, Mozely F (2013) Coal dust in our suburbs: A community-led study of particulate pollution in Newcastle and the Lower Hunter coal train corridor. Coal Terminal Action Group Dust and Health Steering Group: Coal Terminal Action Group. https://www.abc.net.au/cm/lb/5045958/data/dust-data.pdf

Ryan L, Wand M (2014) Re-analysis of ARTC Data on particulate emissions from coal trains. NSW Environment Protection Authority February 25,1-24. https://www.epa.nsw.gov.au/~/media/EPA/Corporate%20Site/resources/air/ARTCreanalysisFeb2014.ashx

Sacks Jason D, Kazuhiko Ito, William E Wilson, and Lucas M Neas (2012) Impact of covariate models on the assessment of the air pollution-mortality association in a single- and multipollutant context. American Journal of Epidemiology 17: 622-34.

Sahu SP, Patra AK (2020) Development and assessment of multiple regression and neural network models for prediction of respirable PM in the vicinity of a surface coal mine in India. Arab J Geosci 13, 890. https://doi.org/10.1007/s12517-020-05771-3

Sahu SP, Pakra AK (2022) Assessment of dispersion of respirable particles emitted from opencast mining operations: development and validation of stepwise regression models. Environment, Development and Sustainability 24:9139–9164. 10.1007/s10668-021-01816-z

Schraufnagel DE (2020) The health effects of ultrafine particles. Exp Mol Med 52, 311–317. https://doi.org/10.1038/s12276-020-0403-3

Shea E, Perera F, & Mills D (2020) Towards a fuller assessment of the economic benefits of reducing air pollution from fossil fuel combustion: Per-case monetary estimates for children's health outcomes. Environmental Research 182, 109019. https://doi.org/10.1016/j.envres.2019.109019

Solé, V. A., E. Papillon, M. Cotte, Ph. Walter, and J. Susini. (2007) A Multiplatform Code for the Analysis of Energy-Dispersive X-Ray Fluorescence Spectra. Spectrochimica Acta Part B: Atomic Spectroscopy 62, no. 1: 63–68. https://doi.org/10.1016/j.sab.2006.12.002.

Spencer-Hwang R, Soret S, Knutsen S, Shavlik D, Ghamsary M, Beeson WL, Kim W, & Montgomery S (2015) Respiratory health risks for children living near a major railyard. Journal of Community Health 40(5), 1015–1023. https://doi.org/10.1007/s10900-015-0026-0

Srivastava A, Kumar A, Elumalai SP (2021) Evaluating Dispersion modeling of inhalable particulates (PM10) emissions in complex terrain of coal mines. Environmental Modeling & Assessment 26:85-403.

Tanrikulu S, Tran C, Beaver S (2011) Health Impact Assessment of Fine Particulate Matter in the Bay Area. Bay Area Air Quality Management District, Research and Modeling Section Publication No 201109-009-PM. September. https://www.baaqmd.gov/~/media/Files/Planning%20and%20Research/Research%20and%20Modeling/Cost%20analysis%20of%20fine%20particulate%20matter%20in%20the%20Bay%20Area.ashx

Tecer LH, Süren P, Alagha O, et al. (2008) Effect of meteorological parameters on fine and coarse particulate matter mass concentration in a coal-mining area in Zonguldak, Turkey. Journal of the Air & Waste Management Association 58:4, 543-552. DOI: 10.3155/1047-3289.58.4.543

Tessum CW, Paolella DA, Chambliss SE, Apte JS, Hill JD, Marshall JD (2021) $PM_{2.5}$ polluters disproportionately and systemically affect people of color in the United States. Science Advances 7(18): eabf4491. https://doi.org/10.1126/sciadv.abf4491

Thurston GD, et al. (2013) NPACT Study 4. Mortality and long-term exposure to $PM_{2.5}$ and its components in the American Cancer Society's Cancer Prevention Study II Cohort. In: National Particle Component Toxicity (NPACT) Initiative: Integrated Epidemiologic and Toxicologic Studies of the Health Effects of Particulate Matter Components. Research Report 177. Health Effects Institute, Boston, MA.

Thurston GD, Awe Y, Ostro B, Sanchez-Triana E (2021) Are All Air Pollution Particles Equal? How Constituents and Sources of Fine Air Pollution Particles ($PM_{2.5}$) Affect Health. World Bank, Washington, DC. World Bank. https://openknowledge.worldbank.org/handle/10986/36269

Trivedi R, Chakraborty MK, Tewary BK (2009) Dust dispersion modeling using fugitive dust model at an opencast coal project of Western Coalfields Limited, India. Journal of Scientific & Industrial Research 68:71-78.

Tsai CJ, Nair U, Hafner H (Eds.) (2020): Low-cost Sensors for Air Quality Monitoring, Aerosol Air Qual Res 20.

Tunno BJ, Sheila Tripathy, Kinnee E, et al. (2018) Fine-scale source apportionment including diesel-related elemental and organic constituents of $PM_{2.5}$ across downtown Pittsburgh. Int J Environ Res Public Health Oct; 15: 2177.

U.S. EPA (2019) Integrated Science Assessment (ISA) for Particulate Matter (Final Report, Dec 2019). U.S. Environmental Protection Agency, Washington, DC. https://cfpub.epa.gov/ncea/isa/recordisplay.cfm?deid=347534

U.S. EPA (2019) Policy Assessment for the Review of the National Ambient Air Quality Standards for Particulate Matter. EPA-452/R-22-004 section 12.5.4. https://www.epa.gov/system/files/documents/2022-05/Final%20Policy%20Assessment%20for%20the%20Reconsideration%20of%20the%20PM%20NAAQS_May2022_0.pdf

U.S. Energy Information Administration (2022, February 15) Coal explained: Mining and transportation of coal. https://www.eia.gov/energyexplained/coal/mining-and-transportation.php

Vedal S, et al. (2013) Section 1. NPACT epidemiologic study of components of fne particulate matter and cardiovascular disease in the MESA and WHI-OS cohorts. In: National Particle Component Toxicity (NPACT) Initiative Report on Cardiovascular Effects, Research Report 178. Health Effects Institute, Boston, MA.

Vohra K, Vodonos A, Schwartz J, Marais EA, Sulprizio MP, & Mickley LJ (2021) Global mortality from outdoor fine particle pollution generated by fossil fuel combustion: Results from GEOS-Chem. Environmental Research 195 110754. https://doi.org/10.1016/j.envres.2021.110754

Wang Y., Xiao S., Zhang Y et al. (2022) Long-term exposure to $PM_{2.5}$ major components and mortality in the southeastern United States. Environment International, 158, art. no. 106969

Wesolowski, J. J., John, W. (1978) Collection Surfaces of Cascade Impactors. X-Ray Fluorescence Analysis of Environmental Samples, edited by T. Dzubay, 121–30. Ann Arbor, MI: Ann Arbor Science Publishers

WHO (2021) WHO global air quality guidelines: particulate matter ($PM_{2.5}$ and PM10), ozone, nitrogen dioxide, sulfur dioxide and carbon monoxide (License: CC BY-NC-SA 3.0 IGO; pp. xxi, 273). World Health Organization, Geneva. https://apps.who.int/iris/handle/10665/345329

Wu PC, Cheng TJ, Kuo CP, Fu JS, Lai HC, Chiu TY, Lai LW (2020) Transient risk of ambient fine particulate matter on hourly cardiovascular events in Tainan City, Taiwan. PlOS One 15(8): e0238082. https://doi.org/10.1371/journal.pone.0238082

Yatkin, Sinan, Claudio A. Belis, Michel Gerboles, Giulia Calzolai, Franco Lucarelli, Fabrizia Cavalli, and Krystyna Trzepla. (2016) An Interlaboratory Comparison Study on the Measurement of Elements in PM10. Atmospheric Environment 125: 61–68. https://doi.org/10.1016/j.atmosenv.2015.10.084.

Yorifuji T, Suzuki E, & Kashima S (2014a) Cardiovascular emergency hospital visits and hourly changes in air pollution. Stroke 45(5), 1264–1268. https://doi.org/10.1161/STROKEAHA.114.005227

Yorifuji T, Suzuki E, & Kashima S (2014b) Hourly differences in air pollution and risk of respiratory disease in the elderly: a time-stratified case-crossover study. Environmental Health 13(1), 67. https://doi.org/10.1186/1476-069X-13-67

Zeger SL, Dominici F, McDermott A, Samet J (2008) Mortality in the Medicare population and chronic exposure to fine particulate air pollution in urban centers (2000-2005). Environ health perspectives 116: 1614-1619.

Zhang X, Zhao L, Tong DQ, Wu G, Dan M, Teng B (2016) A systematic review of global desert dust and associated human health effects. Atmosphere 7(12):158.

8. Appendices

Appendix 1: Section 2 Data Field Descriptions

The following discussion provides more background regarding the data fields, their units, and their calculation.

TrainStart: This field reports the date and time, to the second, that a train was observed by the customized artificial intelligence camera system

TrainType: This study classified the observed trains into four types:

- Passenger – either Amtrak or CalTrain trains
- Freight – Union Pacific trains that are carrying various products on rail cars but not identifiable coal-bearing cars
- Coal – Union Pacific trains exclusively carrying coal hopper rail cars, either full or unloaded

PreTrainPM#: These fields represent the air quality levels before the arrival of a train. We explored various combinations of averaging times (1, 3, 5, and 10 minutes) and gap lengths between the PreTrainPM average and the observed train start time (1, 2, 5, and 10 minutes. For example, PreTrainPM10-10 utilizes a 10-minute average $PM_{2.5, a}$ 10-minute gap between the averaging period, and the train event start. This field is presented in micrograms per cubic meter.

AvgPM This field is the average $PM_{2.5}$ concentration, in micrograms per cubic meter, observed during the time that a train was observed at the monitoring location. Note that each second of recorded data is the average of three separate PM sensors, and this value is in turn the average of those averages.

MaxPM: This field is the maximum 10-second $PM_{2.5}$ concentration, in micrograms per cubic meter, observed during the time that a train was observed at the monitoring location. Again, the data point is the average of three separate PM sensors.

PMdelta_10_10: These fields represent the difference between the $PM_{2.5}$ concentrations observed during the train event and pre-event levels. They are calculated as:

XPM − Pretrain_10_10

where XPM is either the AvgPM or the MaxPM

Miles per hour: This field is the estimated speed of the train using a custom video processing algorithm. The video is separated into individual images. Two positions (x-coordinates) are selected on either side of each image to act as positional triggers. The pixel values (in RGB) are collected from every pixel in each of these two lines. As the trains pass, we anticipate the pixel values to oscillate more than in the rest of the image; therefore, a y-coordinate is chosen with the maximum relative standard deviation out of all the y-coordinates in each line. Since each image is related to a distinct timestamp, we compare the first derivative of pixel intensity change in each optical band (R, G, and B) to find the temporal difference in peaks. Specifically, we are calculating the lag time between the train observed in each of the two locations. The distance between these two points is calculated from a conversion factor of pixels per meter, as determined by image analysis of Amtrak engines and train cars, whose dimensions are publicly available. Knowing the distance traveled (in meters) and the time difference (in seconds), we converted and calculated the speed in meters per second.

Direction: This field indicates the direction the train was traveling in the observation. The determination of this parameter uses the same algorithm described for the previous parameter (m/s). The analyzed derivative peaks inform whether the train is moving to the right (northward and away from the terminal) or left (southward or towards the terminal), resulting in binary values of 1 and 0, respectively.

Appendix 2: Section 2 descriptive statistics for regression

Passenger Trains

Stats	PMave	PMave_C	PMmax10	PMmax10_C	Wind	TS	Humidity	Temp
Mean	.36212	-.15727	9.7675	-.15437	3.11	30.7	70.741	66.29
SD	1.7242	1.5461	7.8401	1.5532	1.40	7.16	15.351	7.673
Min	-18.84	-9.4019	2.5	-9.4019	0	3.6	20	51.3
Max	29.84	13.801	39.75	13.801	8.2	44.3	95	93.1
N	2235	2235	20	20	2235	2235	2235	2235

Freight Trains

Stats	PMave	PMave_C	PMmax10	PMmax10_C	Wind	TS	Humidity	Temp
Mean	4.2347	1.3748	22.745	2.5612	2.84	17.1	76.505	63.84
SD	9.8485	5.2076	31.526	7.3161	1.49	5.7	15.177	8.269
Min	-9.8	-7.057	0	-5.2539	0	1.3	20	49.5
Max	68.46	36.208	157.73	49.002	8.8	38.9	96	100
N	568	568	507	507	568	568	568	568

Full Coal Trains

Stats	PMave	PMave_C	PMmax10	PMmax10_C	Wind	TS	Humidity	Temp
Mean	6.3867	2.5569	24.305	4.2791	3.05	12.8	75.867	62.14
SD	13.3	6.5004	42.809	9.5825	1.64	5.5	16.274	7.929
Min	-.42	-2.5676	1.7	-2.0174	1	6.7	49	53.5
Max	41.43	19.443	162.4	33.68	8.8	29.1	94	76.6
N	15	15	15	15	15	15	15	15

Empty Coal Trains

Stats	PMave	PMave_C	PMmax10	PMmax10_C	Wind	TS	Humidity	Temp
Mean	1.935	1.5673	12.286	1.8331	1.38	15.8	60.286	71.94
SD	4.8405	2.5167	18.95	2.5482	.582	3.2	15.544	6.996
Min	-.57	-1.0231	1.35	-1.0231	.661	10.3	37	58.4
Max	18.54	9	74.3	9	2.73	20.1	84	85.9
N	14	14	14	14	14	14	14	14

Note: PMave = Change in average $PM_{2.5}$ ($\mu g/m^3$); PMave_C = Change in average Corrected $PM_{2.5}$ ($\mu g/m^3$) PMmax10 = Change in peak $PM_{2.5}$ ($\mu g/m^3$); PMmax10_C = Change in peak Corrected $PM_{2.5}$ ($\mu g/m^3$); Wind = Average wind speed (m/s); TS = Train speed (m/s); Temp = Average Temp (F)

Appendix 3: DRUM Sampling methods

Particulate matter (PM) samples were collected using a DRUM-style cascading impactor (Davis Rotating Unit for Monitoring). Samples were deposited on thin (3 μm) Mylar® (biaxially-oriented polyethylene terephthalate) substrates that were lightly greased (Apiezon-L high vacuum grease diluted in Optima grade toluene, 2% wt/v). The application of grease was intended to reduce particle bounce effects resulting in inaccurate particle size profiling (Ihalainen et al., 2012; Wesolowski and John, 1978). The samples were collected semi-continuously at 3-hour temporal resolution in eight discrete size bins via inertial impaction. Specifically:

Stage 1 - inlet to 5.0 μm
Stage 2 - 5.0 to 2.5 μm
Stage 3 - 2.5 to 1.15 μm
Stage 4 - 1.15 to 0.75 μm
Stage 5 - 0.75 to 0.56 μm
Stage 6 - 0.56 to 0.34 μm
Stage 7 - 0.34 to 0.26 μm
Stage 8 - 0.26 to 0.09 μm

The lower cutpoints are controlled by "infinite slot" jets preceding each substrate. The slot width of the jets was confirmed using feeler gauges prior to deployment. A full discussion of the DRUM impaction process can be found in the DRUM Quality Assurance Plan, available at http://delta.ucdavis.edu/DQAP1.pdf.

After each 6-week deployment, the samples were returned to the laboratory at UC Davis. The sample substrates from each stage were removed from the sampling disks and framed on clean, polyethylene frames. Each frame was labeled with descriptions of the samples and stored in a clean acrylic container. The substrates were critically reviewed during the framing process for any signs of contamination or damage (Level 0 validation). Affected samples were recorded in the field notes logbook, and the associated sample data was flagged as invalid.

The prepared samples were analyzed using several non-destructive techniques to determine mass concentrations, optical characteristics, and elemental concentrations. The following sections provide descriptions of each of these methods.

Optical Attenuation via Broadband Spectroscopy

Broadband transmittance/reflectance spectrometry was used to measure the optical attenuation of samples between the wavelengths of 350 and 1050 nm. Broadband light is emitted from both tungsten-halogen and deuterium lamps and then directed toward the sample with a bare fiber optic patch cord. Transmitted light was collected by a focusing lens and detected by a broadband spectrometer (B&W tek i-Trometer, New Jersey, USA). A method to detect reflected light was developed during this project that eliminated multiple reflections due to substrate wrinkles. Sample substrates were scanned before and after sampling. The data reduction and interpretation are still under development and have not been reported with the full data set.

In the data reduction steps, the sampling date is assigned to a specific position along the sample substrate. Dark bands of deposit present decreases in the reflectance as more light is absorbed rather than reflected. The calculation of scattering coefficients from the calibrated reflectance measurements is in progress.

The raw photon counts are converted to inverse megameters, Mm^{-1}, using the Beers-Lambert law, $b_{ext}(\lambda) = -A/V * LN\ [\ (I_{meas}(\lambda) - I_{dark}(\lambda))\ /\ (I_{ref}\ (\lambda) - I_{dark}(\lambda))\ ]$, where $b_{ext}(\lambda)$ is the optical extinction at wavelength λ, A is the sample deposit area in square millimeters, V is the sampled air volume in cubic meters, and $I_x(\lambda)$ is the measured intensities at wavelength λ. The subscript $dark$ refers to measurements made with the polyethylene frame obstructing the optical path. The subscript ref refers to the mean transmission intensity of field blanks. Until a collocated comparison can be performed to accurately assess the uncertainty of the measurement, a conservative 20 % was reported. The method detection limit (MDL) was determined as two times the standard deviation of field blanks, $MDL = 2 * \sigma_{fb}$.

Values are quantified for fourteen wavelengths spanning 350 to 1050 nm wavelengths at 50 nm intervals. The 400 nm wavelength is omitted due to poor detection. The wavelength dependence, or Ångström exponent α, is based on the power law relationship $\tau(\lambda) = \tau_1\lambda^{-\alpha}$. Exponents are calculated and compared for the short (350-450 nm), mid (450-650, nm), and long (650-900 nm) wavelength ranges, as each range has different sensitivities for fine mode radii of aerosols (Ångström, 1929).

Mass Concentration via Soft-Beta Ray Attenuation

Soft-beta ray attenuation was used to quantify mass concentrations of the collected DRUM samples. A Ni-63 radioactive source (λ~100 yr) emits low-energy beta rays (~17 keV) with very short range in matter. The extinction of beta rays through matter is directly proportional to mass via the Beer-Lamber law, $b = Aexp(-\alpha\lambda)$, where b is the extinction of beta rays, A and λ are calibration factors, and α is the areal density of the target. The system is calibrated using multiple thin films of known areal densities.

Elemental Concentrations via Ion Beam Analysis

Elemental characterization using ion beam analysis (IBA) was performed at the UC Davis Crocker Nuclear Lab cyclotron via Proton-Induced X-ray Emission spectroscopy (PIXE) for light elements sodium through zinc, Proton Elastic Scattering Analysis (PESA) for the quantification of bound hydrogen, and Rutherford backscattering for quantification of bound carbon. The cyclotron facility provides high photon flux, which is necessary for the quantification of elemental concentrations from the small sample loadings collected by DRUM impactors.

Characteristic X-rays are induced from each sample by the intense energy beam, 9 MeV H_2^+ protons. The characteristic X-rays emitted by the collected sample deposit were detected by a SII Vortex silicon drift detector (Vortex EX, SII Nano Technology USA). The spectra were modeled using peak fitting software (PyMca, Solé et al., 2007). Calibration is determined by analysis of a mixed set of single- and multi-element reference materials along with several NIST standard reference materials (Yatkin et al., 2016).

Areal densities, x square centimeters, are converted to elemental mass concentrations in nanograms per cubic meter using the beam spot size, S_{beam} square centimeters, and sample air volume, V cubic meters.

$$C_i = x_i * S_{beam} / V \ X \ 1000 \ ng/\mu g$$

Uncertainty and MDLs were calculated using the same method as optical attenuation.

Appendix 4: Section 5 Local Health Statistics

A.4.1 Low birth weight and preterm birth rates for census tracts near coal and petcoke rail, storage, and handling facilities, Richmond, and Contra Costa County and by insurance status, 2016-2021

Metric / Locale	Total (count)	Black	Am. Indian - Alaskan Native	Latinx / Hispanic	Asian	Native Hawaii / Pacific Islander	White	Multi-Race	Other	UK	Medi-Cal	Other Gov. Pgms	Private Insured
Birth Rate													
Study Census Tracts	(1853)	14.31%	*	66.55%	20.00%	*	8.3	*	*	*	37.89% (17.3%, 52.7%)	*	60.19% (39.7%, 84.8%)
Richmond	(3973)	13.1%	*	52.4%	13.3%	0.7%	14.7%	3.3%	*	2.1%	34.2%	2.7%	60.8%
Contra Costa	(34,313)	8.2%	0.1%	32.8%	17.4%	0.7%	32.4%	5.6%	0.2%	2.5%	17.3%	0.8%	80.1%
Low Birth Weight Rate													
Study Census Tracts	8.1% Average (6.2 - 10.4)										*	*	*
Richmond	6.6%	10.8%	*	5.8%	7.2%	*	5.1%	9.0%	*	*	7.70%	13.20%	5.80%
Contra Costa	5.7%	9.5%	*	5.4%	7.4%	8.1%	3.8%	6.7%	*	5.7%	7.50%	16.00%	5.10%
Preterm Birth Rate													
Study Census Tracts	9.4% Average (7.8 - 11.2)										*	*	*
Richmond	8.7%	11.3%	*	9.3%	7.6%	*	5.5%	*	*	*	11.20%	15.10%	7.00%
Contra Costa	7.7%	10.4%	*	8.0%	8.3%	11.4%	6.3%	8.6%	*	7.3%	9.70%	19.20%	7.10%

LBW = Low Birth Weight, birth weight < 2500 grams

Preterm = Obstetric estimate of gestational age at birth < 37 weeks

* Percentages have been suppressed when the number of births with the described characteristics is < 11 to comply with confidentiality constraints

Source: California Comprehensive Birth Files and Reallocation Files 2016-2021 accessed through Vital Registration Business Information System 3/1/2022

A.4.2 Mortality neighborhoods proximate to monitoring sites, Richmond, Contra Costa County, 2016-20

Mortality Rate per 100,000	Total Race & Age Adj	Black	Am. Indian - Alaskan Native	Latinx / Hispanic	Asian / Pacific Islander	Native Hawaiian / Pacific Islander	White	Multi-Race	Other
All Cause Mortality									
Study Site Avg**	787.96	1,500.25	*	258.43	761.25	*	1,471.40	*	*
Richmond	652.05	1,435.83	*	263.59	431.92	1,288.52	979.10	383.75	463.92
Contra Costa	593.69	960.87	974.54	300.58	426.59	834.43	1,024.99	277.78	415.64
All Cancer									
Study Site Avg*	157.77	318.68	*	*	*	*	315.33	*	*
Richmond	138.83	295.4	*	51.9	117.3	*	220.8	59.8	*
Contra Costa	133.13	209.6	289.7	63.8	111.9	207.7	232.9	59.3	153.1
Heart Disease									
Study Site Avg	157.29	372.15	*	*	*	*	*	*	*
Richmond	126.11	310.27	*	42.86	67.00	*	192.14	54.82	*
Contra Costa	108.29	189.38	158.03	49.4	72.04	151.03	196.01	39.63	65.63
Stroke									
Study Site Avg	49.61	106.82	*	*	*	*	*	*	*
Richmond	44.59	92.24	*	16.72	35.89	*	64.39	*	*
Contra Costa	43.53	65.49	*	21.14	42.18	79.29	74.67	10.74	*
Lung Cancer									
Study Site Avg	30.69	*	*	*	*	*	*	*	*
Richmond	25.97	66.15	*	*	21.54	*	45.99	*	*
Contra Costa	25.41	41.51	*	7.80	23.27	41.53	46.27	9.26	*
Chronic Lower Respiratory Disease									
Study Site Avg	19.42	*	*	*	*	*	*	*	*
Richmond	24.94	64.29	*	5.57	*	*	47.01	*	*
Contra Costa	26.06	37.13	*	7.25	9.88	*	53.62	12.22	*
Ischemic Heart Disease									
Study Site Avg	85.36	*	*	*	*	*	*	*	*
Richmond	69.16	162.12	*	25.72	38.29	*	98.11	*	*
Contra Costa	54.62	95.73	*	26.96	40.06	86.84	95.57	24.44	*
Respiratory Disease									
Study Site Avg	75.93	118.69	*	*	*	*	*	*	*
Richmond	48.71	108.08	*	17.57	22.73	*	85.85	*	*
Contra Costa	52.39	71.33	*	20.39	31.13	71.74	99.84	25.93	*

*Cells with < 11 or pop < 20 are not reported. ** Ave is provided when >=t 3 of the census tracts had available data
Decedents of unknown/missing race not included in the race/ethnicity breakdowns but are included in "All race"
Source: Deaths from California Comprehensive Death File and Reallocation File 2016 - 2020 accessed at Vital Registration Business Intelligence System 8/13/21

A.4.3 Rate of emergency department discharges for asthma, and cardiovascular, cerebrovascular, and respiratory conditions by zip codes corresponding to monitoring sites, Contra Costa County; 2016-2020

Rates per 100k	Total	Black**	Am. Indian Alaska Native**	Latinx / Hispanic**	Asian / Pacific Islander**	White**	<1***	<5***	<18***	18+***	65+***
Asthma											
94801	1628.3	3611.6	*	1554.0	359.4	559.7	*	3098.3	2714.8	1250.6	748.5
94804	1229.7	2883.3	*	1185.5	313.1	220.2	*	2431.0	2019.1	994.0	625.8
Contra Costa	554.6	1783.1	691.5	878.2	199.0	252.9	263.3	1008.9	835.3	472.3	256.5
Cardiovascular											
94801	636.7	1903.6	*	394.1	256.7	678.8	*	*	*	852.0	2449.7
94804	604.2	1616.5	*	276.0	328.7	502.7	0.0	*	*	778.4	2255.2
Contra Costa	453.0	811.5	664.2	308.1	213.5	570.9	88.3	10.6	19.0	580.3	1601.2
Cerebrovascular											
94801	125.3	233.8	*	101.9	*	154.8	0.0	*	*	167.2	494.9
94804	118.2	237.2	*	86.0	86.1	90.7	0.0	*	*	152.3	512.0
Contra Costa	93.4	144.8	100.1	82.1	64.3	100.3	*	*	2.2	120.1	362.6
Respiratory											
94801	9878.2	16913.2	2686.6	10040.3	2695.8	3632.0	55174.0	37459.9	17953.4	7071.0	6204.8
94804	7249.5	12320.9	4285.7	8254.7	2610.1	1860.3	35167.8	24573.3	13573.3	5361.2	4494.1
Contra Costa	3876.4	8458.5	4103.7	6510.9	1528.9	2077.5	21856.2	12642.5	6821.1	3013.3	2662.8

Rates are per 100,000 population
*   Rates based on events < 11 or in populations < 30 are not reported based on stability concerns
** Crude Rates - do not take into account the differing age distributions between race/ethnicity groups and should be interpreted with caution   *** Age Specific Rates
Emergency Department discharge data before 2019 did not allow more than one race to be reported, so all visits were assigned a single race code and population denominators with multirace coding were excluded, the rates for single race are thus overestimates and will be biased to the extent that multirace are unevenly distributed amongst those reporting each race first at the emergency department
Emergency Department Discharge data before 2019 used the combined category of "Asian or Pacific Islander" so rates for the combined category are reported here
Rates for "other" race are not included because of differences in determining other for ED visits and population
Sources: Emergency Department Discharge Limited Data Model Data Sets 2016-2020, Office of Statewide Health Planning and Development (OSHPD); American Community Survey 2020 5-year estimates data profiles DP05 (2016-2020), US Census; California Comprehensive Birth File 2018, Vital Records Business Intelligence System (accessed 8/9/2021)

A.4.4 Rates for asthma-related ED visits and hospitalizations in Alameda county (2012-2014)

	West Oakland (zip 94607) Age-adjusted rate (95% LCL-UCL)	Oakland Age-adjusted rate (95% LCL-UCL)	Alameda county Age-adjusted rate (95% LCL-UCL)
Asthma ED rate	1218.4 (1138.3-1298.5)	838.8 (822.6-855.1)	545.8 (539-552.6)
Child (<5) Asthma ED rate	2026.2 (1635.4-2482.2)	1416.4 (1334.2-1498.6)	1053.3 (1016-1090.5)
Asthma hospitalization rate	229.3 (193.2-265.3)	178.9 (171.2-186.5)	112.2 (109.1-115.4)
Child (<5) asthma hospitalization rate	871.5 (622.6-1186.7)	747.3 (687.6-807)	415.4 (392-438.8)

Source: ACPHD 2016